The Astrophysical Journal, 775:104 (28pp), 2013 October 1 doi:10.1088/0004-637X/775/2/104

A BIOMASS-BASED MODEL TO ESTIMATE THE PLAUSIBILITY OF EXOPLANET BIOSIGNATURE GASES

S. Seager[1,2], W. Bains[1,3], and R. Hu[1]
[1] Department of Earth, Atmospheric, and Planetary Sciences, Massachusetts Institute of Technology, 77 Massachusetts Ave., Cambridge, MA 02139, USA
[2] Department of Physics, Massachusetts Institute of Technology, 77 Massachusetts Ave., Cambridge, MA 02139, USA
[3] Rufus Scientific Ltd, 37 The Moor, Melbourn, Royston, Herts SG8 6ED, UK
Received 2012 October 12; accepted 2013 July 7; published 2013 September 12

ABSTRACT

Biosignature gas detection is one of the ultimate future goals for exoplanet atmosphere studies. We have created a framework for linking biosignature gas detectability to biomass estimates, including atmospheric photochemistry and biological thermodynamics. The new framework is intended to liberate predictive atmosphere models from requiring fixed, Earth-like biosignature gas source fluxes. New biosignature gases can be considered with a check that the biomass estimate is physically plausible. We have validated the models on terrestrial production of NO, H_2S, CH_4, CH_3Cl, and DMS. We have applied the models to propose NH_3 as a biosignature gas on a "cold Haber World," a planet with a N_2–H_2 atmosphere, and to demonstrate why gases such as CH_3Cl must have too large of a biomass to be a plausible biosignature gas on planets with Earth or early-Earth-like atmospheres orbiting a Sun-like star. To construct the biomass models, we developed a functional classification of biosignature gases, and found that gases (such as CH_4, H_2S, and N_2O) produced from life that extracts energy from chemical potential energy gradients will always have false positives because geochemistry has the same gases to work with as life does, and gases (such as DMS and CH_3Cl) produced for secondary metabolic reasons are far less likely to have false positives but because of their highly specialized origin are more likely to be produced in small quantities. The biomass model estimates are valid to one or two orders of magnitude; the goal is an independent approach to testing whether a biosignature gas is plausible rather than a precise quantification of atmospheric biosignature gases and their corresponding biomasses.

Key words: astrobiology – planets and satellites: atmospheres

Online-only material: color figures

1. INTRODUCTION

The future detection of signs of life on exoplanets through the detection of atmospheric biosignature gases has been a topic of long-standing interest (e.g., Lovelock 1965). With the push to discover exoplanets of lower and lower masses, the foundation for biosignature gases is becoming more relevant. The sheer variety of exoplanets is furthermore motivating the community to take a broader view of biosignature gases than has been conventionally considered.

1.1. Exoplanet Biosignature Background

The canonical concept for the search for atmospheric biosignature gases is to find a terrestrial exoplanet atmosphere severely out of thermochemical redox equilibrium (Lovelock 1965). Redox chemistry[4] is used by all life on Earth and is thought to enable more flexibility for biochemistry than nonredox chemistry (Bains & Seager 2012). Redox chemistry is also used to capture environmental energy for biological use. The idea is that gas by-products from metabolic redox reactions can accumulate in the atmosphere and would be recognized as biosignature gases because abiotic processes are unlikely to create a redox disequilibrium. Indeed, Earth's atmosphere has oxygen (a highly oxidized species) and methane (a very reduced species), a combination several orders of magnitude out of thermodynamic equilibrium.

In practice, it could be difficult to detect molecular features of two different gases that are out of redox disequilibrium. The Earth as an exoplanet, for example (see Figure 8 in Meadows & Seager 2010), has a relatively prominent oxygen absorption feature at 0.76 μm, whereas methane at present-day levels of 1.6 ppm has only extremely weak spectral features. During early Earth, CH_4 may have been present at much higher levels (1000 ppm or even 1%), as it was possibly produced by widespread methanogenic bacteria (Haqq-Misra et al. 2008, and references therein). Such high CH_4 concentrations would be easier to detect, but because the Earth was not oxygenated during early times, O_2 and CH_4 would not have been detectable concurrently (see Des Marais et al. 2002). There may have been a short period of time in Earth's history when CH_4 levels were high and before the rise of oxygen when both could have been detected (Kaltenegger et al. 2007).

The more realistically identifiable atmospheric biosignature gas from future remote sensing observations is a single gas completely out of chemical equilibrium with the other known or expected atmospheric constituents. Earth's example again is oxygen or ozone, with the oxygen level being about 10 orders of magnitude higher than expected from equilibrium chemistry (Kasting & Walker 1981; Segura et al. 2007; Hu et al. 2012) and having no known abiotic production at such high levels. Although a single biosignature gas may be all that is detectable by future exoplanet atmosphere observations, reliance on a single biosignature gas is more prone to false positives than the detection of two (or more) gases that are out of equilibrium. In the paradigm of detecting signs of life by a single biosignature gas, we still retain the assumption that life uses chemical reactions to extract, store, and release energy, such that biosignature gases are generated as by-products somewhere in life's metabolic process.

How can we decide upon the exoplanet atmosphere gases that are identifiable as biosignature gases? Regardless of the strategy used, only the spectroscopically active, globally mixed gases would be visible in an exoplanet spectrum. Most work

[4] Redox chemistry adds or removes electrons from an atom or molecule (reduction or oxidation, respectively).

to date has focused on conservative extensions of the dominant biosignature gases found on Earth, O_2 (and its photochemical product O_3), and N_2O, as well as the possibility of CH_4 on early Earth. Research forays into biosignature gases that are negligible on present-day Earth but may play a significant role on other planets has started. Pilcher (2003) suggested that organosulfur compounds, particularly methanethiol (CH_3SH, the sulfur analog of methanol) could be produced in high enough abundance by bacteria, possibly creating a biosignature on other planets. CH_3Cl was first considered by Segura et al. (2005) and sulfur biogenic gases on anoxic planets were comprehensively investigated by Domagal-Goldman et al. (2011).

A slight deviation from terracentricity is to consider Earth-like atmospheres and Earth-like biosignature gases on planets orbiting M stars. Segura et al. (2005) found that CH_4, N_2O, and even CH_3Cl have higher concentrations and, therefore, stronger spectral features on planets orbiting quiet M stars compared to Earth. The Segura et al. (2005) work strictly focuses on Earth's production rates for the biosignature gases.[5] The reduced ultraviolet (UV) radiation on quiet M stars enables longer biosignature gas lifetimes and, therefore, higher concentrations to accumulate. Specifically, lower UV flux sets up a lower atmospheric concentration of the OH radical than in Earth's solar UV environment. OH is the major destructive radical in Earth's atmosphere and with less OH, most biosignature gases have longer lifetimes. Seager et al. (2012) have reviewed the range of gases and solids produced by life on Earth.

A necessary new area of biosignature gas research will be predicting or identifying molecules that are potential biosignature gases on super-Earth planets different from Earth. The reasons are twofold. First, the microbial world on Earth is incredibly diverse, and microorganisms yield a broad range of metabolic by-products far beyond the gases called out in exoplanet biosignature research so far. In an environment different from Earth's, these metabolic by-products may accumulate to produce detectable biosignature gases different from those on past and present Earth. Second, while we anticipate the discovery of transiting super-Earths in the habitable zones of the brightest low-mass stars (Nutzman & Charbonneau 2008) and in the future Earths from direct imaging (e.g., Cash 2006; Trauger & Traub 2007; Lawson 2009), the prize targets around bright stars will be rare. It follows that the chance of finding an Earth twin might be tiny and so we must be prepared to identify a wide range of biosignature gases.

In this paper, we take a step forward to expand the possibilities for biosignature gas detection in the future. We provide a quantitative framework to consider biosignature gas source fluxes of any type and any value in any exoplanet environment, via a new biomass model estimate that provides a physical reality plausibility check on the amount of biomass required. This new method liberates modelers from assuming that exoplanet biosignature gas source fluxes are identical to those on Earth.

1.2. Terrestrial Biofluxes

We summarize terrestrial biosignature gas fluxes for later reference as to what is a physically reasonable local ($F_{\rm field}$, in units of mole m^{-2} s^{-1}) and global annual total biosignature gas flux ($\mathcal{F}_{\rm global}$, in units of Tg yr^{-1}). Biological production of gases on Earth are limited by the availability of energy and nutrients. We emphasize that these terrestrial biosignature gas fluxes—which we call field fluxes—are strictly used in this work for consistency checks by comparison with our calculated biosignature gas fluxes.

[5] In effect Segura et al. (2005) and others assume that Earth was transported as is, with its modern atmosphere, oceans, and biosphere, into orbit around an M dwarf star. While this is a useful starting point, it is clearly a very special case.

Table 1
Field Fluxes from Local Environmental Measurements for Select Biosignature Gases

Molecule	Field Flux (mole m^{-2} s^{-1})	Equivalent Global Flux (Tg yr^{-1})	Global Flux (Tg yr^{-1})
CH_3Cl	6.14×10^{-12}	1.5	2–12
COS	1.68×10^{-11}	4.7	...
CS_2	2.10×10^{-10}	7.5	0.1–0.19
DMS	3.61×10^{-10}	105	15–25
H_2S	2.08×10^{-10}	33	0.2–1.6
Isoprene	8.38×10^{-9}	2.7×10^3	400–600
N_2O	5.22×10^{-9}	1.1×10^3	4.6–17
NH_3	...	...	10.7

Notes. The geometric mean of the maximum measured field flux values from different studies are given. Also listed are the equivalent corresponding global fluxes if the maximum field fluxes were present everywhere on Earth's land surface, as well as the actual terrestrial global flux values for comparison. Field flux NH_3 values are not reported because on Earth free NH_3 is negligible as emission from biological systems. Global flux values for COS is absent because soils on average are net absorbers; Watts (2000) report global COS fluxes as 0.35 ± 0.83 Tg yr^{-1}. Field flux measurement references are provided in Table 9 in the Appendix. The global flux references are from Seinfeld & Pandis (2000), with the exception of isoprene which is from Arneth et al. (2008).

For Earth as a whole, the dominant energy-capture chemistry is photosynthesis. Photosynthesis generates around 2.0×10^5 Tg (of oxygen) yr^{-1} (e.g., Friend et al. 2009). The primary carbon production rate from photosynthesis is about 1×10^5 Tg yr^{-1} (Field et al. 1998).

Earth has many biosignature gases beyond photosynthesis-produced O_2. Some of the other biosignature gases can be produced at relatively high flux rates, as listed in Table 1. In Table 1, we list the geometric mean of the maximum field flux from one or more environmental campaigns. The main point is that very high fluxes of biosignature gases can be generated where the surface environment is appropriate (suitable levels of relevant nutrients and energy sources).

We now turn to some specific examples of high terrestrial biosignature gas fluxes. As listed in Table 1, fluxes of some biosignature gases (e.g., isoprene and N_2O) can be very large when extrapolated from their local maximum values to a global total. In addition to the values in Table 1, biogenic NO_x fluxes from natural (unfertilized) environments can be 10–30 ng (N) m^{-2} s^{-1} (Williams et al. 1992; Davidson & Kingerlee 1997), which translates to a global flux across Earth's land surface of ~150 to 300 Tg yr^{-1}. For environments where organic matter, water, and other nutrients are abundant (such as swamps), flux rates of methane can reach 10^4 ng (C) m^{-2} s^{-1} (Prieme 1994; Dalal et al. 2008), which if scaled to a global flux would be 10–20 Pg yr^{-1}. We note, however, that scaling the flux from a swamp, which is rapidly degrading biomass imported from other environments, to a global flux is not realistic, so we do not include these methane rates in Table 1.

Measured field fluxes, $F_{\rm field}$, as presented in the literature vary over many orders of magnitude for the same gas species either within a given study or among different studies. We must therefore take an average of the literature reported $F_{\rm field}$ values and we choose to take the geometric mean of the maximum

Table 2
Laboratory Flux Measurements R_{lab} of Select Biosignature Gases in Units of mole g^{-1} s^{-1}

Molecule	Sea (mole g^{-1} s^{-1})	Seaweed (mole g^{-1} s^{-1})	Land Micro (mole g^{-1} s^{-1})	Land Macro (mole g^{-1} s^{-1})	Adopted Value (mole g^{-1} s^{-1})
N_2O	...	...	9.88×10^{-10}	...	9.88×10^{-10}
NO	...	...	4.57×10^{-10}	...	4.57×10^{-10}
H_2S	1.00×10^{-4}	...	4.69×10^{-7}	...	4.51×10^{-6}
CH_4	2.27×10^{-8}	...	2.92×10^{-6}	...	8.67×10^{-7}
CH_3Br	8.87×10^{-12}	1.04×10^{-14}	...	1.23×10^{-14}	8.87×10^{-12}
CH_3Cl	6.17×10^{-11}	3.04×10^{-15}	...	5.80×10^{-12}	6.17×10^{-11}
COS	1.75×10^{-16}	...	...	3.15×10^{-14}	3.15×10^{-14}
CS_2	2.61×10^{-14}	...	...	...	2.61×10^{-14}
DMS	3.64×10^{-7}	...	2.45×10^{-15}	4.80×10^{-15}	3.64×10^{-7}
Isoprene	4.40×10^{-14}	2.63×10^{-16}	5.61×10^{-10}	9.00×10^{-10}	9.00×10^{-10}

Notes. The adopted R_{lab} are maximum values for Type I biosignature gases (first four rows) and geometric means of the maximum values for Type III biosignature gases (last six rows); see Section 1.2 for more details. Up to dozens of individual studies were considered. Blank entries have no suitable data available in the literature. The categories are "sea": microscopic marine species (phytoplankton, zooplankton, and bacteria); "seaweed": oceanic macroalgal species; "land micro": microscopic land-based species; and "land macro": macroscopic land-based species. Some values were reported in the literature per gram of dry weight. Conversion from dry to wet weights was performed according to the following fraction dry weight/wet weight: seaweed = 0.18 (Nicotri 1980); bacteria = 0.35 (Bratbak & Dundas 1984; Simon & Azam 1989); phytoplankton = 0.2 (Ricketts 1966; Omori 1969); fungi = 0.23 (Bakken & Olsen 1983); lichen = 0.45 (Lang et al. 1976; Larson 1981); and land plants (green, not woody) = 0.3 (Chandler & Thorpe 1987; Black et al. 1999). The laboratory flux measurement references are provided in Table 10 in the Appendix.

F_{field} values reported in each study. We choose to use the maximum of the field fluxes for a given study because the maximum represents the ecology with the maximum number of gas-producing organisms in an environment where they are producing gas with maximal efficiency, and a minimum density of non-producing organisms and gas-consuming organisms. The huge variation in measured F_{field} is due to different growth conditions, different nutrient and energy supply, and different diffusion rates. It is important to note that the biomass of bioflux-producing organisms in the field is rarely measured. Because the field fluxes are measured from an ecosystem with a range of organisms other than the bioflux-producing organisms, in some cases the biosignature gas of interest is consumed before it reaches the atmosphere. To take an average of all of the maximum field fluxes from different studies for a given organism, we use the geometric mean (of the maximum).

The geometric mean is the appropriate average of concentrations of processes limited by energy. There is a log relationship between concentration and the energy needed to drive a reaction:

$$\Delta G = -RT \ln(K), \quad (1)$$

where G is the Gibbs free energy, R is the universal gas constant, T is temperature, and K is the equilibrium constant. To properly compare a set of concentrations produced by metabolism requiring energy, the logs of the concentrations are appropriate. For R_{lab} just as for F_{field}, we take the geometric mean of the maxima of each study. We choose the maximum observed rate because it represents the closest approximation to the case where the organisms are dependent on the gas-generating reaction for the majority of their energy.

The bioflux produced by laboratory cultures is also relevant for exoplanet biomass calculations, in addition to the above described field fluxes. We call the lab-measured metabolic by-product production rate per unit mass R_{lab}, in units of mole g^{-1} s^{-1}. The R_{lab} values of a variety of biosignature gases are listed in Table 2. R_{lab} is used for validation of the biomass models and as input into one of the biomass models (see Section 3.3). The R_{lab} measurements are an important complement to field measurements as they are made on pure cultures of known mass, unlike the mixed culture of unknown mass in the field. A summary of different flux definitions is provided in Table 3.

Table 3
Definition of Fluxes

Flux	Definition	Units
$\mathcal{F}_{global}$	Global flux	Tg yr^{-1}
F_{source}	Field or biosignature flux	mole m^{-2} s^{-1}
R_{lab}	Lab culture flux	mole g^{-1} s^{-1}
P_{m_e}	Minimal maintenance energy rate	kJ g^{-1} s^{-1}

The lab production rates R_{lab} vary by several orders of magnitude. The variation in lab production rates is in part due to differences in the organisms studied in the lab, but mainly due to different laboratory conditions, especially growth conditions (nutrient concentration, temperature, and other environmental factors such as whether the organisms are stressed by stirring or shaking, non-natural light levels or spectra, or the presence or absence of trace chemicals such as metal ions). For R_{lab} for biological reactions based on energy extraction from the environment (defined as Type I biosignature gases; see Section 2.1), we again use the geometric mean as an average quantity of R_{lab}, because the energy released is related to the log of the concentration of the reactants and products (see above). For biological reactions that do not extract energy from the environment (defined as Type III biosignature gases; see Section 2.3), we use the maximum value of R_{lab}. Their production rate is determined by the ecology of the organism. Ecological factors include the chemical environment of the species and the presence of other species, which are rarely mimicked accurately in the laboratory. As a result laboratory production is likely to be very substantially lower than that in the wild. We therefore take the maximum flux found in the laboratory measurement of Type III biosignature gas production as being the nearest approximation to the natural flux capacity.

1.3. Terrestrial Biomass Densities

We summarize terrestrial biomass surface densities for later reference as to what is a reasonable biomass surface density. For our exoplanet biomass model use and validation, we require an understanding of the range of biomass surface densities on Earth. Based on life on Earth, a summary overview is that a biomass surface density of 10 g m^{-2} is sensible, 100 g m^{-2} is plausible, and 5000 g m^{-2} is possible. Real-world situations are nearly always limited by energy, bulk nutrients (carbon, nitrogen), trace nutrients (iron, etc.), or all three.

We distinguish active biomass from inactive biomass. Active biomass is the mass of organisms metabolizing at a sufficiently high rate to grow (see ahead to the discussion on the microbial minimal maintenance energy consumption rate in Section 3.1.2). Most terrestrial environments contain an excess of material that is biologically derived but is not actively metabolizing. For example, the mass of organic material in soil is 10–100 times greater than the mass of actively metabolizing microorganisms (e.g., Anderson & Domsch 1989; Insam & Domsch 1988). Some of this organic material is dormant organisms but most is the remains of dead organisms (bacteria, fungi, and plants). In the following paragraphs, we are concerned solely with the surface density of active biomass—the biomass actively generating by-product gases.

We now turn to some specific examples of biomass surface densities on Earth.

Photosynthesizing marine microorganisms are the dominant life over the majority of the surface area of Earth. Their biomass is limited by phosphate, nitrogen, iron, and other micronutrients (because there is no "soil" in the surface of the deep ocean from which to extract micronutrients), and reaches 5–10 g m^{-2} on the ocean surface (Ishizaka et al. 1994; Karl et al. 1991; Mitchell et al. 1991). Adding nutrients can boost the photosynthesizing marine microorganism surface density to 50 g m^{-2} or more (Bishop et al. 2002; Buesseler et al. 2004; Boyd et al. 2000).

The biomass surface densities for ocean life described above are all in about the top 10 m of water, i.e., the well-mixed surface zone. Nearly all of the active ocean biomass is in the top layers of the ocean, both photosynthetic organisms and their predators. The above ocean biomass estimates do not include the biomass in the deep ocean, where light does not penetrate. Deep-living organisms must gain their energy either from the small amount of biological material that falls from the photosynthetic layer above, or from rare geochemical energy sources, such as ocean ridge or mantle hot-spot volcanic sites. While deep heterotrophs and hot-spot geotrophs are of great conceptual importance in our understanding of the range of environments in which life can exist, their contribution to the total active biomass of the Earth is not dominant.

Microbial biofilms are limited by nutrients, energy, and space. Films on seashores, in rivers, in acid mine drainage have a huge range of organism surface densities ranging from 0.1 g m^{-2} to 10 g m^{-2} (MacLulich 1987; Lawrence et al. 1991; Neu & Lawrence 1997; Gitelson et al. 2000). Densities of 1000 g m^{-2} or more can be achieved if very high density of nutrients are provided, as, for example, in agricultural waste water (Gitelson et al. 2000).

The mass of actively metabolizing microorganisms in soil is approximately[6] 100–200 g m^{-2} (Olsen & Bakken 1987; Anderson & Domsch 1989). Energy-generating nutrients are probably limiting in this case: if unlimited energy-generating substrates are provided to fungi, as occurs, for example, in commercial mushroom farming, densities of >20,000 g m^{-2} can be reached routinely (Shen et al. 2002).

Actively metabolizing land plant tissue has surface densities varying from 0 to over 5000 g m^{-2}, depending on the availability of energy and nutrients. Densities of 5000–10,000 g m^{-2} of active biomass are achieved in environments where sunlight provides unlimited energy and nutrients are provided in excess, for example, in modern agriculture settings (Brereton 1971; Hamilton & Bernier 1975). Densities of 100 g m^{-2} are more typical of productive grasslands.

We do not include trees or forests in our biomass density comparisons. While forests are visually very obvious, high-density accumulations of organic carbon, nearly all of that carbon is relatively metabolic inactive. Wood (formally, secondary xylem) acts as a passive mechanical support for trees and a conduit for transport of water and nutrients between the metabolically active leaves and root surfaces. Wood produces negligible amounts of metabolic product on its own. As most of a tree is wood, it is an inappropriate comparison for active microbial or algal biomass. Nevertheless, for comparison, tree biomass densities of $\sim 6.0 \times 10^4$ g m^{-2}, of which 1%–5% represents actively metabolizing green matter, are common in mature temperate forests (Whittaker 1966).

We do not include the deep rock biosphere in our estimates of biomass density, as (as far as is known today) crustal subsurface life has minimal direct effect on the atmosphere. In the last decade, organisms have been found in deep crustal rocks that use geochemical sources of energy for growth. The amount of this ecology is unknown—some suggest that there is as much life in the crust as on its surface (Gold 1992). However, crustal life's direct impact on the atmosphere is not obvious. Subsurface life had remained undiscovered for so long because it does not impinge on the surface with gases, soluble molecules, or other obvious indicators that the subsurface organisms are present. The subsurface organisms can only be found by drilling into the rocks. A review of a number of studies of microbial communities found in deep drill rock samples (Pedersen 1993), shows that there are 10^2–10^4 microorganisms g^{-1} of rock. Most studies look at bore-hole water. Typically water from deep (>1 km) bore-holes contains 10^3–10^5 organisms ml^{-1}, and the water probably makes up 2%–4% of the rock by mass (i.e., organism density in the total rock is around 10–10^3 cells g^{-1}). Actual biomass surface densities will depend on how thick the inhabited rock layer is. Any extrapolation of these figures to the possible deep rock microbial community elsewhere on Earth, let alone on an exoplanet, must be speculative.

Closing with a total biomass on Earth estimate, the total amount of carbon on Earth as in cellular carbon in prokaryotes is estimated as $3.5–5.5 \times 10^{14}$ kg (Whitman et al. 1998; Lipp et al. 2008).

1.4. A New Biosignature Approach

The main goal of this paper is the presentation of a biomass model estimate that ties biomass surface density to a given biosignature gas surface source flux. The motivating rationale is that with a biomass estimate, biosignature gas source fluxes can be free parameters in model predictions, by giving a physical plausibility check in terms of reasonable biomass. The new approach enables consideration of a wide variety of both gas species and their atmospheric concentration to be considered in biosignature model predictions. In the future when biosignature

[6] If 100–200 g of microorganisms seems high, note that a 1 m^2 of soil 10 cm deep weighs ~200 kg.

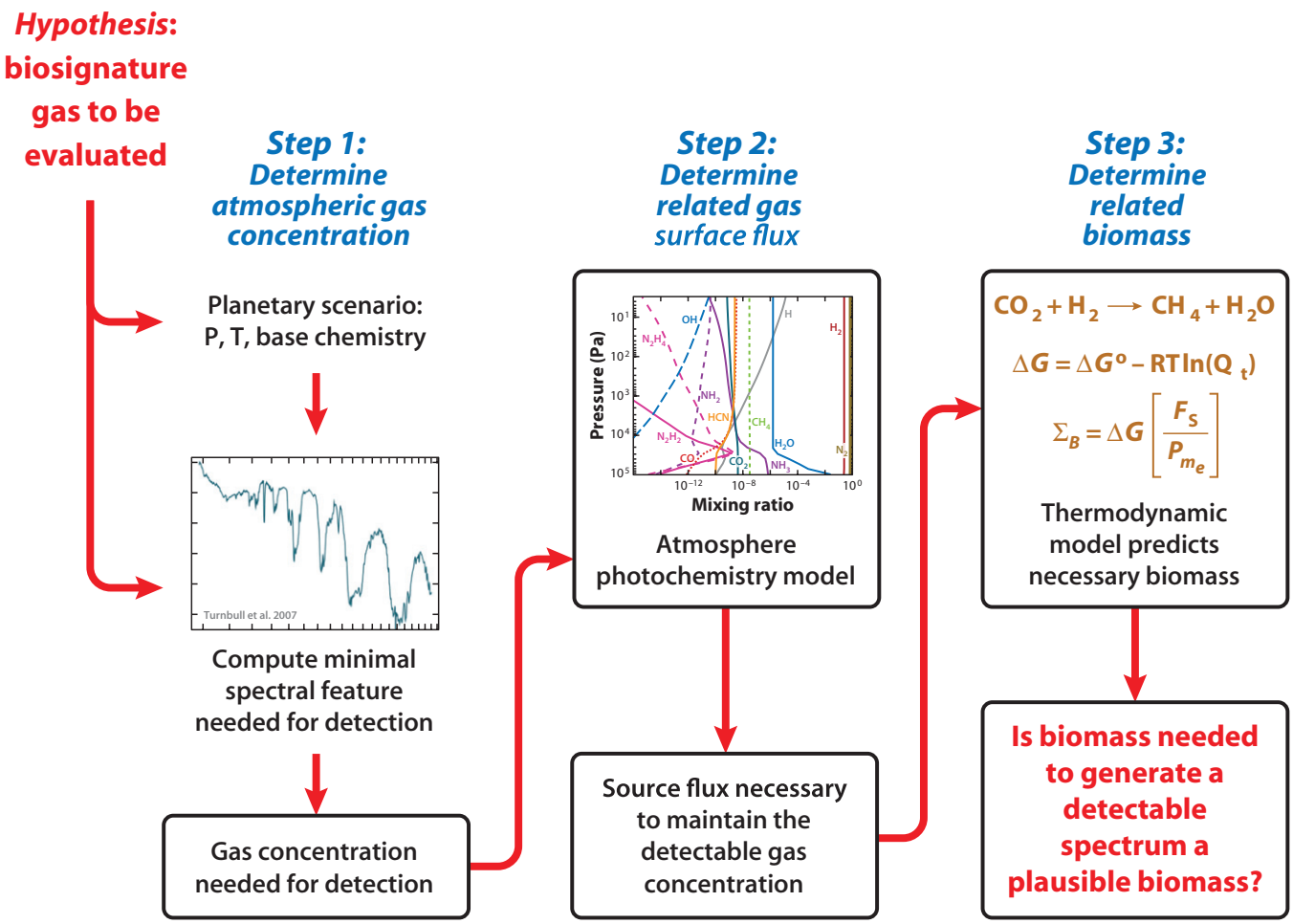

Figure 1. Flowchart description of the use of biomass model estimates. See Section 1.4.
(A color version of this figure is available in the online journal.)

gases are finally detected in exoplanet atmospheres, the biomass model estimate framework can be used for interpretation.

We argue that in order to explore the full range of potential exoplanet biosignature gases, the biosignature gas source flux should be a fundamental starting point for whether or not a biosignature gas will accumulate in an exoplanet atmosphere to levels that will be detectable remotely with future space telescopes. Instead, and until now, biosignature gas fluxes are always adopted as those found on Earth or slight deviations thereof (see Section 1.1 for references), and could not be considered as a free parameter because there is no first principles theoretical methodology for determining the biosignature gas source fluxes. In lieu of a first principles approach, we present model estimates which depend on both the amount of biomass and the rate of biosignature gas production per unit biomass. See Figure 1.

Our proposed approach for biosignature gas studies is to

1. calculate the amount of biosignature gas required to be present at "detectable" levels in an exoplanet atmosphere from a theoretical spectrum (we define a detection metric in Section 4.3);
2. determine the gas source flux necessary to produce the atmospheric biosignature gas in the required atmospheric concentration; the biosignature gas atmospheric concentration is a function not only of the gas surface source flux, but also of other atmospheric and surface sources and sinks (Section 4.1);
3. estimate the biomass that could produce the necessary biosignature gas source flux (Section 3);
4. consider whether the estimated biomass surface density is physically plausible, by comparison to maximum terrestrial biomass surface density values (Section 1.3) and total plausible surface biofluxes (Section 1.2).

We begin in Section 2 with a categorization of biosignature gases into three classes, needed for the respective biomass model estimates presented in Section 3. In Section 4, we describe our atmosphere and photochemistry models used to determine both the required biosignature gas concentration for theoretical detection and the lifetimes of biosignature gases that are produced at the planet surface. In Section 5, we present our results followed by a discussion in Section 6 and a summary in Section 7.

2. BIOSIGNATURE GAS CLASSIFICATION

A classification of biosignature gases based on their origin is needed to develop appropriate biomass models. We make the following definitions. Type I biosignature gases are generated as by-product gases from microbial energy extraction. The Type I biosignature gas biomass model is based on thermodynamics. Type II biosignature gases are by-product gases produced by the

metabolic reactions for biomass building and require energy. There is no useful biomass model for Type II biosignature gases because once the biomass is built a Type II biosignature gas is no longer generated. Type III biosignature gases are produced by life but not as by-products of their central chemical functions. Type III biosignature gases appear to be special to particular species or groups of organisms, and require energy for their production. Because the chemical nature and amount released for Type III biosignature gases are not linked to the local chemistry and thermodynamics, the Type III biosignature gas biomass model is an estimate based on field fluxes and lab culture production rates. We further define *bioindicators* as the end product of chemical reactions of a biosignature gas.

2.1. Type I Biosignature Gas: Redox Gradient Energy Extraction By-product

We define Type I biosignatures as the by-product gases produced from metabolic reactions that capture energy from environmental redox chemical potential energy gradients. Terrestrial microbes can capture this potential energy also described as in the form of chemical disequilibria (we also favor the term "dark energy"). Specifically, chemotrophic organisms couple energetically favorable pairs of oxidation and reduction half-reactions. The disequilibria can involve either completely inorganic compounds or can make use of organic matter. In fact the only clear limitations upon the types of reactions used are that they have a negative Gibbs free energy, and that life can make the reactions occur faster than the rate of non-biological reactions. In other words, Earth-based metabolic pathways exploit chemical energy potential gradients in the form of chemical reactions that are thermodynamically favorable but kinetically inhibited (see, e.g., Madigan et al. 2003 for more details).

The canonical Type I biosignature gas discussed for exoplanets is CH_4 produced from methanogenesis (e.g., Des Marais et al. 2002 and references therein). Methanogens at the sea floor can use H_2 (released from rocks by hot water emitted from deep sea hydrothermal vents (serpentinization)) to reduce CO_2 (available from atmospheric CO_2 that has dissolved in the ocean and mixed to the bottom) resulting in CH_4 and H_2O,

$$H_2 + CO_2 \rightarrow CH_4 + H_2O. \quad (2)$$

Methanogens also use molecules other than H_2 as reductants (including organic molecules). For a description of volatile Type I biosignature gases produced by Earth-based microbes (including H_2, CO_2, N_2, N_2O, NO, NO_2, H_2S, SO_2, and H_2O), see the review by Seager et al. (2012).

On Earth many microbes extract energy from chemical energy gradients using the abundant atmospheric O_2 for aerobic oxidation,

$$X + O_2 \rightarrow \text{oxidized X}. \quad (3)$$

For example, H_2O is generated from H_2, CO_2 from organics, SO_2 or SO_4^{2-} from H_2S, rust from iron sulfide (FeS), NO_2^- and NO_3^- from NH_3, etc.

Turning to an exoplanet with a H-rich atmosphere, the abundant reductant is now atmospheric H_2 such that

$$H_2 + X \rightarrow \text{reduced X}. \quad (4)$$

The oxidant must come from the interior. In other words, for chemical potential energy gradients to exist on a planet with a H-rich atmosphere, the planetary crust must (in part) be oxidized in order to enable a redox couple with the reduced atmosphere. The by-product is always a reduced gas, because in a reducing environment H-rich compounds are the available reductants. Hence, H_2S is expected from SO_2, CH_4 from CO or CO_2, etc. To be more specific, oxidants would include gases, such as CO_2 and SO_2:

$$H_2 + \text{oxidant} \rightarrow CH_4 \text{ or } NH_3 \text{ or } H_2O. \quad (5)$$

The by-product gases are typically those already present in thermodynamical equilibrium. Life only has the same gases to work with as atmospheric chemistry does.

False positives[7] for redox by-product gases are almost always a problem because nature has the same source gases to work with as life does. Furthermore, while in one environment a given redox reaction will be kinetically inhibited and thus proceed only when activated by life's enzymes, in another environment with the right conditions (temperature, pressure, concentration, and acidity), the same reaction might proceed spontaneously. Methane, for example, is produced geologically and emitted from mid-ocean floor ridges. Only a reduced gas that has accumulated to significant, unexpected levels, because the gas has a very short atmospheric lifetime, would be a candidate biosignature gas in an oxidized environment. Alternatively, the presence of reduced biosignature gases (such as CH_4) in an oxidized atmosphere will stand out as candidate biosignature gases (Lederberg 1965; Lovelock 1965); but compare the comments in Section 1 about the potential simultaneous observability of reduced and oxidized gases.

2.2. Type II Biosignature Gas: Biomass Building By-product

We define Type II biosignatures as by-product gases produced by the metabolic reactions for biomass building. On Earth these are reactions that capture environmental carbon (and to a lesser extent other elements) in biomass. Type II biosignature reactions are energy-consuming, and on Earth the energy comes from sunlight via photosynthesis. On Earth photosynthesis captures carbon for biomass building,

$$H_2O + CO_2 \rightarrow CH_2O + O_2, \quad (6)$$

where CH_2O represents sugars. O_2 is Earth's most robust biosignature gas because it is very hard to conceive of geochemical processes that would generate a high partial pressure of oxygen in an atmosphere with CO_2 in it at Earth's atmospheric temperature, making the probability that oxygen is a "false positive" signal very low (Selsis et al. 2002; Segura et al. 2007; Hu et al. 2012). It is, however, easy to explain why life produces oxygen in an oxidized environment. In order to build biomass in an oxidized environment, where carbon is tied up as carbonates or CO_2, living organisms have to generate a highly oxidized by-product in order to reduce CO_2 to biomass. The most plausible oxidized species is molecular oxygen itself. For more subtleties about why building biomass in an oxidizing environment results in a Type II biosignature gas that is more oxidized than the equilibrium atmospheric components, see the detailed discussion in Bains & Seager (2012).

Other potential-oxidized Type II biosignature gases might include volatiles that are oxidized forms of nitrogen (nitrogen oxides) or halogens (molecular halogens, halogen oxides, or halates; see Haas 2010 regarding chloride photosynthesis), all other common elements that could form volatile chemicals

[7] A biosignature gas false positive is a gas produced by abiotic means that could be attributed to production by life.

are completely oxidized in Earth's surface environment. The oxidized forms of nitrogen or halogens are less likely Type II biosignature gases than oxygen itself, as they are all more reactive (and hence damaging to life) than molecular oxygen, require more energy to generate from environmental chemicals, or both.

On a planet with a reduced atmosphere, we can generally state

$$H_2O + CH_4 \rightarrow CH_2O + H_2, \quad (7)$$

$$CO_2 + H_2O + NH_3 \rightarrow CH_2O.N + H_2, \quad (8)$$

etc. Here, the right-hand side has CH_2O as an approximate storage molecule. Because H_2 is the by-product gas—already abundant in an H-rich atmosphere—there are no useful Type II by-product candidate biosignature gases. For further discussion on biosignature gases in a H_2-rich atmosphere see Seager et al. (2013).

2.3. Type III Biosignature Gas: Secondary Metabolic By-product

We define Type III biosignatures as chemicals produced by life for reasons other than energy capture or the construction of the basic components of life. Type III biosignature gases have much more chemical variety as compared to Type I or Type II biosignature gases because they are not the products of reactions that are executed for their thermodynamic effect out of chemicals that exist in the environment. Rather, Type III biosignature gases have a wide variety of functions, including defense against the environment or against other organisms, signaling, or internal physiological control. Like Type II biosignature gases, energy is required to generate Type III biosignature gases.

There are a wide range of Type III biosignatures, including sulfur compounds (e.g., DMS, OCS, CS_2; see Domagal-Goldman et al. 2011), hydrocarbons, halogenated compounds (e.g., CH_3Cl; see Segura et al. 2005, CH_3Br), and a variety of volatile organic carbon chemicals (including isoprene and terpenoids). These products are sometimes called the products of secondary metabolism. See Seager et al. (2012) for a summary.

The most interesting aspect of secondary metabolism gas by-products as a biosignature class is the much more diverse range of molecules than produced by gas products from energy extraction (the Type I biosignature gases). Just as importantly, Type III biosignatures are not as prone to confusion by abiotic false positives as Type I biosignatures. As specialized chemicals, most are not naturally occurring in the atmosphere. Because they require energy and specific catalysis to be produced, Type III biosignature gases are unlikely to be made geologically in substantial amounts, and so are unlikely to be present in the absence of life. In general, the more complicated a molecule is (i.e., the more atoms it has) and the further from fully oxidized or reduced the molecule is, the less are produced by geological sources as compared to more simple molecules. For example, volcanoes produce large quantities of CO_2, somewhat smaller amounts of CH_4, small amounts of OCS, trace amounts of CH_3SH, and none of isoprene. The downside to Type III biosignatures is that because they are usually such specialized compounds they typically are produced in small quantities that do not accumulate to levels detectable by remote sensing.

Type III biosignatures are not directly tied to the environment and therefore could be produced by life on any exoplanet.

2.4. Bioindicators

Biosignature gases can be transformed into other chemical species abiotically. The resulting product might also not be natural occurring in a planet's atmosphere and therefore also a sign of life. We call these abiotically altered products "bioindicators" and consider them a separate subclass of each of the above three types of biosignature gases.

O_3 is a canonical bioindicator derived from the Type II biosignature O_2 (Leger et al. 1993). O_3 is a photochemical product of O_2 (governed by the Chapman cycle; Chapman 1930). As a nonlinear indicator of O_2, O_3 can be a more sensitive test of the presence of O_2 under low atmospheric O_2 conditions (Leger et al. 1993). Other bioindicators that have been described in the literature include ethane (a hydrocarbon compound) from biogenic sulfur gases (Domagal-Goldman et al. 2011) and hazes generated from CH_4 (Haqq-Misra et al. 2008).

3. BIOMASS MODEL

The main goal of this paper is a quantitative connection between global biosignature gas source fluxes and a global biomass surface density estimate. In this way, in models of exoplanet spectra, the biosignature gas source fluxes can be free parameters and checked to be physically plausible via the biomass model estimates. Such a plausibility check is meant to enable study of a wide variety of candidate biosignature gases in both gas species and atmospheric concentration to be considered. The discussion of biosignature flux rates and hence of biosignature detectability can thus be liberated from the requirement of assuming Earth-like biosignature gas source fluxes. We emphasize that we are trying to test whether a biosignature gas can be produced by a physically plausible biomass and we are not trying to predict what a biosphere would look like.

3.1. Type I Biomass Model

3.1.1. Type I Biomass Model Derivation

The biomass surface density for Type I biosignatures can be estimated by conservation of energy. We may equate the required energy rate for organism survival to the energy generation rate from an energy-yielding reaction. The organism survival energy requirements come from an empirical measurement of so-called minimal maintenance energy rate that depends only on temperature (Tijhuis et al. 1993). We describe the minimal maintenance energy rate, P_{m_e}, in units of kJ g^{-1} s^{-1} (i.e., power per unit mass)[8] later in this section. The energy yield rate comes from the Gibbs free energy of the energy-yielding reaction times the rate at which a group of organisms processes the reaction. The Gibbs free energy of the reaction is denoted by ΔG, in units of kJ $mole^{-1}$. The metabolic by-product gas production rate per unit mass is described by R in units of mole g^{-1} s^{-1}. The conservation of energy per unit mass and time is then described by

$$P_{m_e} = \Delta G R. \quad (9)$$

The equation tells us that under the assumption that the energy yield ΔG is used only for maintenance, the by-product gas production rate per unit mass R can be constrained if P_{m_e} is known. The by-product gas production rate is what we have been calling the biosignature gas surface flux.

[8] We use g as a proxy for g of wet weight.

The biomass surface density is the parameter of interest and so we break down R into a biomass surface density Σ_B and a biosignature gas source flux $F_{\rm source}$

$$R = \frac{F_{\rm source}}{\Sigma_B}, \tag{10}$$

where Σ_B is the biomass surface density in g m^{-2}. The biosignature gas source flux $F_{\rm source}$ (in units of mole m^{-2} s^{-1}) describes the surface flux emitted as the metabolic by-product and is also used as an input in a computer model of an exoplanet atmosphere. An important point for exoplanet atmospheres is that $F_{\rm source}$ cannot be directly converted into a detectable gas concentration that makes up a spectral feature—any source flux coming out of a planet surface is usually modified by atmospheric chemical reactions including photochemical processes. In atmosphere modeling, a photochemistry model is needed to translate the source flux into the amount of gas that accumulates in an exoplanet atmosphere. (False positives in the form of geologically produced source fluxes must be also be considered; see Section 6.5.)

The biomass estimate follows from Equations (9) and (10),

$$\Sigma_B \simeq \Delta G \left[\frac{F_{\rm source}}{P_{m_e}}\right]. \tag{11}$$

The free parameter in this biomass estimate equation is the biosignature gas source flux $F_{\rm source}$, because the Gibbs free energy is known and minimal maintenance energy rate is empirically adopted (Section 3.1.2). A caveat is that both ΔG and P_{m_e} depend on temperature.

Σ_B is an apparent minimum biomass surface density estimate because $F_{\rm source}$ may be weakened to a net biosignature gas surface flux if some of the gas is consumed by other organisms. See Section 6.3 for a discussion.

We review the point that ΔG depends on gas concentration. The energy available to do work depends on the concentration of both the reactants and products via

$$\Delta G = \Delta G_0 + RT \ln(Q_t). \tag{12}$$

Here, ΔG_0 is the "standard free energy" of the system (Equation (1)), i.e., the free energy available when all the reactants are in their standard state, one molar concentration (for solutes) or one atmosphere pressure (for gases). R in this context is the universal gas constant and T is temperature. The reaction quotient Q_t is defined as

$$Q_t = \frac{[A]^n[B]^m}{[X]^o[Y]^p}, \tag{13}$$

for the reaction

$$oX + pY \rightarrow nA + mB, \tag{14}$$

where, e.g., $[X]$ is the concentration or partial pressure of species X. In general, care must be taken for the Type I biomass calculations described in this paper as relates to the appropriate ΔG. Most of our ΔG are taken from Amend & Shock (2001).

The biosignature gas source flux, $F_{\rm source}$, can now be used as a free parameter in exoplanet model atmosphere calculations, whereby, again, the purpose of the biomass estimate from Equation (11) is to ensure the biomass surface density underlying the source flux is physically reasonable.

3.1.2. The Minimal Maintenance Energy Consumption Rate, P_{m_e}

We now turn to discuss the microbial minimal maintenance energy consumption rate, P_{m_e}, in more detail. Although P_{m_e} is not yet a familiar quantity in exoplanets research, it is both measured empirically and tied to thermodynamics. P_{m_e} is a fundamental energy flux central to the biomass estimate. P_{m_e} is the minimal amount of energy an organism needs per unit time to survive in an active state (i.e., a state in which the organism is ready to grow). An empirical relation has been identified by Tijhuis et al. (1993) that follows an Arrhenius law

$$P_{m_e} = A \exp\left[\frac{-E_A}{RT}\right]. \tag{15}$$

Here, $E_A = 6.94 \times 10^4$ J mol^{-1} is the activation energy, $R = 8.314$ J mol^{-1} K^{-1} is the universal gas constant, and T in units of kelvin is the temperature. The constant A is 3.9×10^7 kJ g^{-1} s^{-1} for aerobic growth and 2.2×10^7 kJ g^{-1} s^{-1} for anaerobic growth (Tijhuis et al. 1993). Here, per g refers to per gram of wet weight of the organism. Note that we have explicitly converted from Tijuis' P_{m_e} units of kJ (mole C)$^{-1}$ yr^{-1} in bacterial cells to kJ g^{-1} s^{-1} per organism by dividing the P_{m_e} values by a factor of 60 (molecular weight of carbon (=12) $\times$ the ratio of dry weight to carbon (=2) $\times$ the ratio of wet weight to dry weight in bacteria (=2.5)).

The P_{m_e} maintenance energy rate equation (Equation (15)) is species independent (Tijhuis et al. 1993) and also applicable for different microbial culture systems (Harder 1997). The equation is not intended to be very precise, the confidence intervals are 41% and 32% for aerobic and anaerobic growth, respectively (Tijhuis et al. 1993).

P_{m_e} as measured is not strictly a minimal energy requirement. P_{m_e} is in fact the minimal energy needed for a bacterial cell to keep going under conditions under which it is capable of growth. The P_{m_e} is measured during growth, and is extrapolated to growth =0. This extrapolated P_{m_e} is nevertheless not the same as "maintenance energy" for non-growing cells. Growing cells have a variety of energy-required mechanisms "turned on" which non-growing cells will turn off to save energy, such as the machinery to make proteins, break down cell walls, and so on. P_{m_e} as a maintenance energy rate therefore separates out the baseline energy components from the energy needed to actually build biomass. P_{m_e} is therefore the minimal energy needed to maintain active biomass.[9] See Hoehler (2004) for a more detailed review of the different types of "maintenance energy" and their relationship to organism growth.

The P_{m_e} (Equation (15)) is an Arrhenius equation and it is natural to ask why the microbial maintenance energy rate follows Arrhenius' law. Organisms use energy for repair and replacement of damaged molecular components. Molecular damage is caused by non-specific chemical attack on the components of the cell by water, oxygen, and other reactive small molecules. The rate of such reactions is no different than other chemical reactions—well described by an Arrhenius equation. In aggregate, therefore, the overall rate of breakdown of the

[9] We note that this active biomass may be accompanied by a much larger mass of dormant organisms (and an even larger mass of dead ones, as in terrestrial soils). However, dormant and dead organisms will not be significant generators of biosignature gases, and so we are not interested in them for our present study. Equally, we are not interested in dormant organisms' lower energy requirements.

Table 4
Type I Biomass Model Validation for Select Biosignature Gases

Gas	$R_{\rm lab}$ (mole (g^{-1} s^{-1}))	ΔG (kJ $mole^{-1}$)	T (K)	P_{m_e} (kJ (g^{-1} s^{-1}))	Approx. $\frac{R_{\rm lab}\Delta G}{P_{m_e}}$	$\frac{R_{\rm lab}\Delta G}{P_{m_e}}$
N_2O	3.36×10^{-8}	443.7	302	...	...	...
NO	5.36×10^{-9}	355.9	302	...	...	...
N_2O/NO	8.73×10^{-8}	...	302	2.2×10^{-5}	3.2	0.62
H_2S a	8.17×10^{-5}	27.2	338	4.2×10^{-4}	5.3	5.2
H_2S b	6.57×10^{-3}	13.4	374	4.8×10^{-3}	19	19
H_2S c	1.13×10^{-6}	31.8	308	3.8×10^{-5}	0.95	4.8
CH_4	4.7×10^{-5}	191.8	338	4.2×10^{-4}	21	21

Notes. The maintenance energy production rate P_{m_e} should be comparable to the lab production rate fluxes times the free energy $R_{\rm lab}\Delta G$. Averaged values for each literature study are given for $R_{\rm lab}$, Δ_G, and P_{m_e} (T is within a few degrees for each row), with the approximate validation using these averages given in Column 6. The actual validation given in Column 7 is an average of individual values (not shown) of $R_{\rm lab}$, Δ_G, and P_{m_e}. The biosignature gas-producing reactions are listed in the text but can be summarized as N_2O: produced via ammonia oxidation, H_2S a and b: sulfur reduction with H_2, H_2S c: S_2O_3 disproportionation to H_2S, and CH_4: produced via methanogenesis (see the text in Section 3.1.3) for details.

macromolecular components of the cell is expected to follow Arrhenius' law. Arrhenius' law describes chemical reaction rates (indeed any thermally activated process) and has two reaction-specific parameters A and E_A. For two stable molecules to react, chemical bonds need to be broken. E_A, the activation energy of a reaction, represents the energy needed to break the chemical bonds. In uncatalyzed reactions, E_A comes from the thermal energy of the two reacting molecules, which itself follows from the Boltzmann velocity distribution. The probability that any two colliding molecules will have a combined energy greater than E_A is $\exp[-E_A/RT]$. The parameter A is an efficiency factor that takes into account that molecules have to be correctly oriented in order to react.

3.1.3. Type I Biomass Model Validation

Tests of the biomass model for Type I biosignature gases aim to both validate the model and understand the intended range of model accuracy. Because our end goal is to estimate whether the flux of gas necessary to generate a spectral signature is plausible, we aim only for an order of magnitude estimate of the biomass that is producing the biosignature gas of interest.

The first test is to check our basic assumption of conservation of energy in Equation (9) that the maintenance energy rate (P_{m_e}) is approximately equal to the redox energy yield rate ($R_{\rm lab}\Delta G$), via lab-measured rate values. We consider the biosignature gases and corresponding reactions described below and compare the maintenance energy rate to the redox energy yield rate, along with the values for $R_{\rm lab}$, ΔG, and P_{m_e} at the temperature, T, considered (each of these three quantities are temperature-sensitive). To validate using Equation (9), we have averaged the validation results from different literature studies. In other words, we used the appropriate concentration, pH, and temperature for the ΔG and the appropriate temperature for P_{m_e} with the validation result shown in the last column in Table 4. To provide overview values for each individual parameter, Table 4 also shows averaged values for each of $R_{\rm lab}$ and ΔG.

We consider four different Type I biosignature gas-generating reactions. These reactions are selected because they involve the reaction of geochemically available starting materials, have well-characterized microbial chemistry, and for which sufficient $F_{\rm field}$ and $R_{\rm lab}$ measurements are available.

The first reaction is ammonia oxidation to nitrogen oxides, described by

$$2NH_4^+ + 2O_2 \rightarrow N_2O + 3H_2O + 2H^+ \qquad (16)$$
$$4NH_4^+ + 5O_2 \rightarrow 4NO + 6H_2O + 4H^+.$$

We note that the oxidation of ammonia is only a relevant route for production of N_2O in an environment containing molecular oxygen. In both laboratory systems and real ecosystems, organisms oxidize ammonia to N_2O and to NO at the same time, the ratio depending on oxygen availability and other environmental factors. To validate our estimates of gas flux based on energy requirements, we therefore have to account for an organism's production of N_2O *and* NO, as the production of both of these gases contributes materially to the organism's energy budget. For ammonia oxidation, we summed the $R_{\rm lab}\Delta G$ for NO and N_2O generation for each experiment and calculated the geometric mean of those summed values.

Our second, third, and fourth validation examples are for H_2S, a gas produced by many biological reactions. As examples, we choose the reduction of elemental sulfur (at two different temperatures),

$$H_2 + S \rightarrow H_2S, \qquad (17)$$

and the disproportionation of thiosulfate,

$$S_2O_3^{2-} + H_2O \rightarrow HSO_4^{2-} + H_2S. \qquad (18)$$

These two reactions can use geochemically produced substrates, and hence are not dependent on pre-existing biomass.

We choose as a fifth example methanogenesis, via the reduction of CO_2 by H_2 to produce CH_4. Methanogenesis is a key energy-capturing reaction in hydrothermal environments, and a reaction which relies only on geochemical inputs,

$$CO_2 + 4H_2 \rightarrow 2H_2O + CH_4. \qquad (19)$$

Methanogenesis is discussed at length in Sections 5.2 and 5.3.

The validation results—that the lab-based redox energy yield rate compares to the maintenance energy rate within an order of magnitude—are shown in Table 4 (rightmost column). The results show a reasonable confirmation of our application of the minimal maintenance energy concept to biosignature gas production rates to within about an order of magnitude with

one exception. An order of magnitude is expected because of uncertainties in the individual factors: P_{m_e} a factor of two, the gas flux typically a factor of two, and the biomass measurement and conversion values a factor of two.

We pause to discuss the relevance of validating the P_{m_e} equation against lab production rates, given that Tijhuis et al. (1993) already used laboratory measurements in the original paper. The Tijhuis et al. (1993) equation for P_{m_e} (Equation (15)) was developed from studies in which all the inputs and outputs from energy metabolism were completely characterized, so that the energy balance of the organisms could be calculated exactly. The organisms' growth rate was also controlled, so that the energy consumption at zero growth (P_{m_e}) could be inferred directly from the data. In our application we wish to infer the biomass from a single measure of gas output, from organisms whose rate of growth is not known. We therefore needed to validate that such an extrapolation of the application of the P_{m_e} concept is valid.

Based on the lab and P_{m_e} comparison in Table 4, the rate of production of gas in growing cultures of organism in the laboratory is higher than that predicted by the P_{m_e} calculations. This is expected. P_{m_e} is the minimal maintenance energy—the energy needed to maintain the cell in a state ready to grow. Actual growth requires additional energy to assemble cell components. This extra energy demand in turn requires that the cell produce more Type I metabolic waste products per unit mass than is expected from the P_{m_e} calculations. The amount of the excess will depend on specifics of the growth conditions (e.g., what nutrients are supplied to the organisms), the organisms growth rate, and specifics of its metabolism. Thus, Table 4 is consistent with our model, showing that organisms use at least the P_{m_e} of energy in cultures capable of active growth.

Now we comment more specifically on the actual validation numbers in Table 4. Two of the test validation results are too high, at a factor of 20 when they should be close to unity. Based on this high value and reasons described further below, the Type I biomass model should only be used for temperatures below ∼343 K, because the Tijhuis et al. (1993) P_{m_e} equation was derived from measurements taken between 283 and 338 K (with one measurement at 343 K). Both of the anomalously high values in Table 4 are for cultures grown at the upper end of this temperature range. It is possible that at such extreme temperatures organisms require more energy for stress and damage response than predicted from culture at lower temperature. We note that the deviation of P_{m_e} as compared to $\Delta G R_{\rm lab}$ may also be reflected in the temperature dependencies: P_{m_e} follows an exponential with T, whereas ΔG changes linearly with T (Equation (1)).

As a second test of the Type I biomass model, we check the biomass estimate equation (11), specifically that the quantity of interest, the biomass surface density (Σ_B) is reasonable based on the field fluxes, and ΔG and P_{m_e}. In other words, for this second test, we ask if the surface biomass (estimated via Equation (11)) is reasonable by comparison with Earth-based biomass surface densities for the microbial redox energy equation and environment in question. For the N_2O and H_2S examples given above, we find biomass surface densities are below 0.0024 g m^{-2}, as shown in Table 5, well within a plausible biomass surface density (Section 1.3).

We did not validate CH_4 for surface biomass density because maximum local field fluxes of methane are not meaningful for comparison with other gas fluxes in our analysis. Extremely high CH_4 fluxes can be generated from anaerobic biomass breakdown (fermentation), but these represent the rapid breakdown on biomass that has been accumulated over much wider areas and over substantial time. As an extreme example, sewage processing plants can generate substantial methane, but only because they collect their biomass from an entire city. This flux does not therefore represent a process that could be scaled up to cover a planet.

Table 5
Type I Biomass Model Validation for Biomass Surface Density for Select Biosignature Gases

Gas	P_{m_e} (kJ (g^{-1} s^{-1}))	ΔG (kJ mole^{-1})	T (K)	$F_{\rm field}$ (mole (m^{-2} s^{-1}))	Σ_B (g m^{-2})
N_2O/NO	4.1×10^{-5}	−472.0	303	5.22×10^{-9}	2.4×10^{-2}
H_2S a	1.1×10^{-3}	−46.7	338	2.08×10^{-10}	9.3×10^{-6}
H_2S b	1.1×10^{-2}	−48.3	373	2.08×10^{-10}	9.4×10^{-7}
H_2S c	9.5×10^{-5}	−23.9	307	2.08×10^{-10}	5.1×10^{-5}

Notes. The biomass surface density is computed by the Type I biomass model equation (11) using the geometric means of the maximum values of the field fluxes $F_{\rm field}$. The biomass surface density should be reasonable as compared to terrestrial values described in Section 1.3.

We also did not validate the biosignature gas NH_3 because no natural terrestrial environment emits detectable amounts of ammonia on a global scale. NH_3 is sometimes generated by the breakdown of biomass, especially protein-rich biomass or nitrogen-rich excretion products, but NH_3 represents a valuable source of nitrogen, which is taken up rapidly by life. Because ammonia is very soluble in water, any residual NH_3 not taken up by life remains dissolved in water and does not generate any significant amount of NH_3 gas in the atmosphere.

We conclude this subsection by summarizing that the Type I biomass model is a useful estimate to about an order of magnitude. This is validated from our use of the minimum maintenance energy P_{m_e} as compared to lab flux values ($\Delta G R_{\rm lab}$). We also showed that a reasonable biomass surface density is derived using the field flux values in the main Type I biomass equation (Equation (11)).

3.2. Lack of Type II Biosignature Biomass Model

We do not propose a biomass model for Type II biosignature gases and here we explain why. Type II biosignature gases are produced as a result of biomass building. Once the biomass is built, there is no further Type II biosignature gas produced, to a reasonable approximation.

If one wanted to estimate a Type II biosignature gas flux, one would have to estimate the turnover rate of the biomass, which itself depends on seasonality, burial rates, predation, fire clearance, and many other factors. If a turnover rate, Tr, could be determined, then the flux of a Type II biosignature gas would be $Tr \times s$, where s is the stoichiometrically determined amount of biosignature gas needed to generate a gram of biomass. For plants, for example (∼80% water, ∼20% dry weight; of that dry weight 45% is carbon), the stoichiometry of carbon fixation is

$$CO_2 + H_2O \rightarrow CH_2O + O_2, \quad (20)$$

(in other words, one mole of carbon fixed gives one mole of oxygen released), and so $s = 5.6 \times 10^{-3}$ moles O_2 g^{-1} wet weight of plant.

For our present purposes, in the absence of any good framework for estimating exoplanet Tr, we omit biomass models for Type II biosignature gases.

3.3. Type III Biosignature Biomass Estimates

Type III biosignature gases have no physically based biomass model because Type III biosignatures are not linked to the growth or maintenance of the producing organism. Because the amount of biosignature gas produced is arbitrary from the point of view of its overall metabolism, there can be no quantitative biomass model for Type III biosignature gases.

We therefore instead construct a biomass estimate from a framework based on terrestrial Type III biosignature gas fluxes. While tying the biomass estimate to the specifics of terrestrial metabolism is unsatisfactory, it is still more general than the conventional adoption of Earth-like environmental flux rates which assume both terrestrial metabolism and terrestrial ecology. With our Type III biomass estimate approach, we can scale the biosignature gas source flux to different biomass densities that are not achieved on Earth.

3.3.1. Type III Biomass Estimate

In lieu of a quantitative, physical biomass model, we adopt a comparative approach for a biomass estimate. We use the biosignature source fluxes and production rates of Type III metabolites of Earth-based organisms.

We estimate the biomass surface density by taking the biosignature gas source flux $F_{\rm source}$ (in units of mole m^{-2} s^{-1}) divided by the mean gas production rate in the lab $R_{\rm lab}$ (in units of mole g^{-1} s^{-1}), as in Equation (10),

$$\Sigma_B \simeq \frac{F_{\rm source}}{R_{\rm lab}}. \quad (21)$$

Recall that the source flux is measured in the field on Earth (and in that context called $F_{\rm field}$) but assumed or calculated for exoplanet biosignature gas detectability models (and called $F_{\rm source}$). See Table 1 for a list of select Type III field fluxes and Table 2 for a list of select Type III lab rates. As described in Section 1.2, we take the geometric mean of the maximum for the Type III $R_{\rm lab}$ rates $F_{\rm field}$ values from different studies.

The caveat of the Type III biomass estimate explicitly assumes that the range of R for life on exoplanets is similar to that for life in Earth's lab environment.

3.3.2. Type III Biomass Estimate Validation

We now turn to a validity check of the Type III biomass estimate. To validate, we compare the flux rates of Type III biosignature gases observed in the field ($F_{\rm field}$) with the production rate of Type III gases from laboratory culture ($R_{\rm lab}$) of pure organisms. The field rates give a flux per unit area, and the laboratory rates give a flux rate per unit mass. Also, the lab rates are from single species, whereas the field rates are from an ecology. We wish to confirm that comparison of the two predicts a physically plausible biomass per unit area to explain the field flux. We use the values for $F_{\rm field}$ and $R_{\rm lab}$ as given in Table 6.

Most of the Type III biomass surface density values (as shown in Table 6) are well within the values of biomass density seen in natural ecosystems (Section 1.3). We can therefore say that using laboratory fluxes is a reasonable way to approximately estimate the biomass necessary to generate biosignature gas fluxes. We emphasize approximate, because the biomass densities are somewhat high for Type III organism biomass densities.

Table 6
Type III Biomass Estimate Validation

Molecule	$F_{\rm field}$	$R_{\rm lab}$	$\Sigma_B = \frac{F_{\rm field}}{R_{\rm lab}}$
CH_3Cl	2.90×10^{-12}	6.17×10^{-11}	0.0047
COS	1.68×10^{-11}	2.70×10^{-14}	620
CS_2	3.96×10^{-12}	2.61×10^{-14}	150
DMS	5.83×10^{-12}	3.64×10^{-07}	1.6×10^{-5}
Isoprene	8.38×10^{-9}	9.00×10^{-10}	9.3

Notes. The biomass surface density, Σ_B as generated from the Type III biomass in Equation (21). Here, $F_{\rm field}$ are Earth values—the geometric mean of the maximum fluxes from values reported in the literature, taken from Table 1. $R_{\rm lab}$ are Earth lab values, the maximum fluxes from literature studies, and are taken from Table 2.

The biomass surface density validation for COS is somewhat large at 622 g m^{-2}. The problem with COS is that it is both given off and absorbed by ecosystems, often by the same ecosystem at different times. The net field flux may therefore be poorly defined, perhaps representing the release of stored gas. In addition, COS is usually only produced by organisms in response to attack by other organisms such that COS is produced in large quantities in soils but produced in much smaller quantities in lab cultures. The same argument applies to CS_2 and also gives rise to a somewhat large biomass. In any case, COS and CS_2 are examples of how the Type III biomass model based on scaling is approximate only.

The biomass surface density validation for DMS is much lower than the other Type III biomass estimates in Table 6. All of the molecules in the table except DMS are produced at a cost to the organism for carbon and energy in order to perform specific signaling or defense functions. DMS, in contrast, is a product of the consumption of DMSP. DMSP is produced in response to stress and then is broken down enzymatically to DMS by zooplankton. In the lab, DMSP is often fed to the phytoplankton at a level unavailable in the natural environment, and the phytoplankton consume the DMSP at a very high rate likely leading to the high lab DMS production rates, and hence the low biomass surface density estimate.

4. ATMOSPHERE AND PHOTOCHEMISTRY MODEL

A model for atmospheric chemistry is required to connect the concentration of a biosignature gas in the atmosphere as required for detection to the biosignature source flux at the planetary surface. (In turn we use the biosignature source flux to estimate the biomass through the models introduced in Section 3.) The focus on chemistry is critical, because atmospheric sinks that destroy the putative biosignature gas are critical for the gas lifetime and hence accumulation in the planetary atmosphere.

4.1. Photochemistry Model

We aim to calculate the source flux $F_{\rm source}$ or in photochemistry model jargon, the production rate P of a gas species of interest. The production rate is tied to the loss rate L and the steady-state gas concentration $[A]$, via

$$P = L[A]. \quad (22)$$

The source flux is described by

$$F_{\rm source} = \int_z P(z) + \Phi_{\rm dep}, \quad (23)$$

Table 7
Reaction Rates with H, OH, and O of Select Type III Biosignature Gases

Reaction	A	n	E	$T = 270$ K	$T = 370$ K	$T = 470$ K
$DMS + H \rightarrow CH_3SH + CH_3$	4.81×10^{-18}	1.70	9.00	2.63×10^{-24}	2.11×10^{-22}	2.91×10^{-21}
$CH_3Cl + H \rightarrow CH_3 + HCl$	1.83×10^{-17}	0	19.29	1.97×10^{-24}	1.46×10^{-22}	1.92×10^{-21}
$CH_3Br + H \rightarrow CH_3 + HBr$	8.49×10^{-17}	0	24.44	1.59×10^{-21}	3.01×10^{-20}	1.63×10^{-19}
$CH_3I + H \rightarrow CH_3 + HI$	2.74×10^{-17}	1.66	2.49	7.67×10^{-18}	1.75×10^{-17}	3.09×10^{-17}
$DMS + OH \rightarrow CH_3SCH_2 + H_2O$	1.13×10^{-17}	0	2.10	4.43×10^{-18}	5.71×10^{-18}	6.60×10^{-18}
$CH_3Cl + OH \rightarrow CH_2Cl + H_2O$	1.40×10^{-18}	1.60	8.65	2.54×10^{-20}	1.89×10^{-19}	3.17×10^{-19}
$CH_3Br + OH \rightarrow CH_2Br + H_2O$	2.08×10^{-19}	1.30	4.16	2.87×10^{-20}	7.13×10^{-20}	1.30×10^{-19}
$CH_3I + OH \rightarrow CH_2I + H_2O$	3.10×10^{-18}	0	9.31	4.90×10^{-20}	1.50×10^{-19}	2.86×10^{-19}
$DMS + O \rightarrow CH_3SO + CH_3$	1.30×10^{-17}	0	−3.40	5.91×10^{-17}	3.93×10^{-17}	3.10×10^{-17}
$CH_3Cl + O \rightarrow CH_2Cl + OH$	1.74×10^{-17}	0	28.68	1.77×10^{-23}	8.77×10^{-22}	8.26×10^{-21}
$CH_3Br + O \rightarrow CH_2Br + OH$	2.21×10^{-17}	0	30.76	1.77×10^{-23}	8.77×10^{-22}	8.26×10^{-21}
$CH_3I + O \rightarrow CH_3 + IO$	6.19×10^{-18}	0	−2.84	2.19×10^{-17}	1.56×10^{-17}	1.28×10^{-17}

Notes. Second-order reaction rates in units of m^3 molecule^{-1} s^{-1} are computed from the formula $k(T) = A(T/298)^n \exp(-E/RT)$, where T is the temperature in K and R is the gas constant ($R = 8.314472 \times 10^{-3}$ kJ mole^{-1}). The reactions rate are compiled from the NIST Chemical Kinetic Database.

where z is altitude and Φ_{dep} is the deposition flux described later below.

The derivation of the production rate (source flux) equation is as follows. In steady state,

$$\frac{d[A]}{dt} = P - L[A] = 0, \quad (24)$$

where $[A]$ is the number density of species A (in units of molecule m^{-3}), P is the production rate of species A (in units of molecule m^{-3} s^{-1}), and L is the loss rate of species A in (in units of s^{-1}). By rearranging Equation (24), we have $P = L[A]$. We also note that the loss rate is often described by its inverse, the lifetime of an atmospheric gas

$$t = \frac{1}{L}. \quad (25)$$

The loss rate can be described in more detail. The loss rate can be due to reactions with other species B, as in

$$L[A] = K_{AB}[A][B], \quad (26)$$

where K_{AB} is the second-order reaction rate in units of m^3 molecule^{-1} s^{-1}. Values of K_{AB} are presented in Table 7 for gases studied in this paper. The loss rate can also be due to photochemical dissociation of species A, as in

$$L[A] = J[A] = \int_\lambda q_\lambda I_\lambda \exp^{-\tau_\lambda} \sigma_\lambda [A] d\lambda, \quad (27)$$

where J is the photodissociation loss rate, q_λ is the quantum yield, I_λ is the stellar intensity, $\exp^{-\tau_\lambda}$ is the attenuation by optical depth τ_λ, σ is the photodissociation cross section of the species A, and λ is wavelength. Photodissociation is most relevant high in the atmosphere typically above mbar levels to which stellar UV radiation can penetrate from above.

Gases can be lost from the atmosphere by deposition to the ground. This loss is at the surface only (and numerically is treated as a lower boundary condition), in contrast to the photochemical loss rate reactions which take place throughout the upper atmosphere. Dry deposition is deposition onto a surface (either solid land or liquid water oceans) and wet deposition is deposition into water (rain) droplets (Seinfeld & Pandis 2000).

The deposition velocity at the planetary surface can be described by

$$\Phi_{dep} = n v_d, \quad (28)$$

where Φ is the molecular loss flux at the surface due to dry deposition, n is the number density (in units of molecules m^{-3}) at the surface of the species under consideration, and v_d is the dry deposition velocity (in units of m s^{-1}). The wet deposition is relevant for water-soluble gases and is not usually described as a velocity but as a process that occurs throughout the layer where water condenses (on Earth the troposphere) (Hu et al. 2012). Where photochemical reactions are slow, the deposition rate (the rate of loss to the ground) can control the atmospheric concentration of gas. Surface deposition consists of two processes: transfer of a gas between the atmosphere and the surface and removal of the gas from the surface. The rate of transfer from the atmosphere to the surface is proportional to the concentration difference between the atmosphere and the surface. Thus, once transferred to the surface, the gas has to be chemically removed, or the surface will saturate with gas, there will be no more transfer—the deposition rate will be zero. The values of wet and dry deposition velocities can be measured on Earth (e.g., Sehmel 1980), but the wet and dry deposition rates for various gases are highly variable and therefore averages tend to be used in models.

Caution must be taken, however, in applying Earth-based averages to exoplanets. The chemistry that removes many of Earth's atmospheric gases at the surface, such as methane, ammonia, OCS, and methyl chloride from Earth's atmosphere are biochemical, not geochemical. Life actively consumes these gases. So deposition rates on exoplanets may be very different from those in the terrestrial atmosphere. We discuss this in more detail in the context of CH_4 and NH_3 in Sections 5.2 and 5.1, respectively. In summary, caution should be taken when extrapolating the Earth-measured values to planetary applications. Notably, if the surface is saturated with a specific molecule, the surface uptake of the molecule may be reduced to zero.

The production rate are written in terms of the two different loss rates (and considering Φ_{dep} as a surface boundary

condition),

$$P = [A](J + K_{AB}[B]). \quad (29)$$

The production rate is here assumed to be from biological sources, but when considering false positives, the geological source should also be considered.

For biosignature gases that are minor chemical perturbers in the atmosphere, the biosignature lifetime can be estimated based on the dominant loss rate via Equation (26). The simplified example for one species A gets more complicated for the case where there are several terms in the loss rate and when the production rate also includes other chemical reactions, and this is where the photochemistry model calculation is required. The steady-state concentration $[B]$ is unknown and calculating $[B]$ is one reason why a full photochemical model is needed to go beyond estimates.

The full photochemical model is presented in Hu et al. (2012). The photochemical code computes a steady-state chemical composition of an exoplanetary atmosphere. The system can be described by a set of time-dependent continuity equations, one equation for each species at each altitude. Each equation describes chemical production, chemical loss, eddy diffusion and molecular diffusion (contributing to production or loss), sedimentation (for aerosols only), emission and dry deposition at the lower boundary, and diffusion-limited atmospheric escape for light species at the upper boundary. The code includes 111 species, 824 chemical reactions, and 71 photochemical reactions.

Starting from an initial state, the system is numerically evolved to the steady state in which the number densities no longer change. Because the removal timescales of different species are very different, an implicit inverse Euler method is employed for numerical time stepping. The generic model computes chemical and photochemical reactions among all O, H, N, C, and S species, and formation of sulfur and sulfate aerosols. The numerical code is designed to have the flexibility of choosing a subset of species and reactions in the computation. The code therefore has the ability to treat both oxidized and reduced conditions, by allowing selection of "fast species." For the chemical and photochemical reactions, we use the most up-to-date reaction rate data from both the National Institute of Standards and Technology (NIST) database (http://kinetics.nist.gov) and the JPL publication (Sander et al. 2011). UV and visible radiation in the atmosphere is computed by the δ-Eddington two-stream method with molecular absorption, Rayleigh scattering, and aerosol Mie scattering contributing to the optical depth.

We developed the photochemistry model from the ground up from basic chemical and physical principles and using both established and improved computer algorithms (see Hu et al. 2012 and references therein). We tested and validated the model by reproducing the atmospheric composition of Earth and Mars. For one of the tests, we simulated Earth's atmosphere starting from an 80% N_2 and 20% O_2 atmosphere and temperature profile of the US Standard Atmosphere 1976. Important atmospheric minor species are emitted from the lower boundary by standard amounts (e.g., reported by the IPCC), including CO, CH_4, NH_3, N_2O, NO_x, SO_2, OCS, H_2S, and H_2SO_4. We validate that vertical profiles predicted by our photochemical model of O_3, N_2O, CH_4, H_2O, OH, HO_2, NO, NO_2, and HNO_3 match with various balloon and satellite observations, and the surface mixing ratios of OH, O_3, SO_2, and H_2S also match with standard tropospheric values (see Hu et al. 2012, for details). As another test, we reproduce the chemical composition of the current Mars atmosphere, in agreement with measured compositions (e.g., Krasnopolsky 2006) and previous one-dimensional photochemistry model results (e.g., Zahnle et al. 2008). In particular, the code correctly illustrates the effect of HO_x catalytic chemistry that stabilizes Mars' CO_2-dominated atmosphere, predicting an O_2 mixing ratio of $\sim$1500 ppb.

4.2. Atmosphere Model

We compute synthetic spectra of the modeled exoplanet's atmospheric transmission and thermal emission with a line-by-line radiative transfer code (Seager et al. 2000; Miller-Ricci et al. 2009; Madhusudhan & Seager 2009). Opacities are based on molecular absorption with cross sections computed based from the HITRAN 2008 database (Rothman et al. 2009), molecular collision-induced absorption when necessary (e.g., Borysow 2002), Rayleigh scattering, and aerosol extinction computed based on Mie theory. The transmission is computed for each wavelength by integrating the optical depth along the limb path, as outlined in, e.g., Seager & Sasselov (2000). The planetary thermal emission is computed by integrating the radiative transfer equation without scattering for each wavelength (e.g., Seager 2010).

The temperature profiles for the simulated atmospheres are self-consistently computed with the gray-atmosphere assumption (Guillot 2010). Opacities of CO_2, H_2O, CH_4, O_2, O_3, OH, CH_2O, H_2O_2, HO_2, H_2S, SO_2, CO, and NH_3 are considered, if they are needed in the atmospheric scenario under consideration. For the gray-atmosphere temperature profiles, we have assumed isotropic irradiation, and applied the convection correction if the radiative temperature gradient is steeper than the adiabatic lapse rate. We have assumed for all cases the planetary Bond albedo is 0.3; in other words, we have implicitly assumed a cloud coverage of 50% (assuming cloud albedo to be 0.6). For consistency, we account for the effect of clouds on the planetary reflection and thermal emission spectrum by a weighted average of spectra with and without clouds as in Des Marais et al. (2002).

We emphasize that the precise temperature–pressure structure of the atmosphere is less important than photochemistry for a first-order description of biosignature gases.

4.3. Detection Metric

We now describe our metric for a "detection" that leads to a required biosignature gas concentration. For now, the detection has to be a theoretical exercise using synthetic data. We determine the required biosignature gas concentration based on a spectral feature detection with an SNR = 10. Specifically, we describe the SNR of the spectral feature as the difference between the flux in the absorption feature and the flux in the surrounding continuum (on either side of the feature) taking into account the uncertainties on the data,

$$\mathrm{SNR} = \frac{|F_{\mathrm{out}} - F_{\mathrm{in}}|}{\sqrt{\sigma_{F_{\mathrm{out}}}^2 + \sigma_{F_{\mathrm{in}}}^2}}, \quad (30)$$

where $F_{\mathrm{in}} \pm \sigma_{F_{\mathrm{in}}}$ is the flux density inside the absorption feature and $F_{\mathrm{out}} \pm \sigma_{F_{\mathrm{out}}}$ is the flux density in the surrounding continuum, and σ is the uncertainty on the measurement.

The uncertainties of the in-feature flux and continuum flux are calculated for a limiting scenario: an Earth-sized planet orbiting a noiseless Sun-like star at 10 pc observed (via direct imaging) with a 6 m diameter telescope mirror operating within 50%

of the shot noise limit and a quantum efficiency of 20%. The integration time is assumed to be 20 hr. We note that collecting area, observational integration time, and source distance are interchangeable depending on the time-dependent observational systematics.

5. RESULTS

Our results are the biomass estimates for exoplanet atmosphere scenarios with select biosignature gases. We present a few case studies, including both familiar biosignature and bioindicator gases and biosignature gases not yet widely discussed. The illustrative examples are for thermal emission spectra. A later paper also treats transmission spectra (Seager et al. 2013). The case studies aim to demonstrate the use of the biomass model: to take a biosignature gas, let the source flux be a free parameter (instead of tied to Earth-life production rates), and check that the biomass is physically plausible.

5.1. NH_3 as a Biosignature Gas in a Reducing Atmosphere

We propose ammonia, NH_3, as a biosignature gas in a H_2-rich exoplanet atmosphere. NH_3 is a good biosignature gas candidate for any thin H_2-rich exoplanet atmosphere because of its short lifetime and lack of production sources. NH_3 as a biosignature gas is a new idea, and one that is specific to a non-Earth-like planet. On Earth, NH_3 is not a useful biosignature gas because, as a highly valuable molecule for life that is produced in only small quantities, it is rapidly depleted by life and unable to accumulate in the atmosphere.

The biosignature idea is that ammonia would be produced from hydrogen and nitrogen, in an atmosphere rich in both,

$$3H_2 + N_2 \rightarrow 2NH_3. \quad (31)$$

This is an exothermic reaction which could be used to capture energy. We propose that in a H_2-rich atmosphere, life can catalyze breaking of the N_2 triple bond and the H_2 bond to produce NH_3, and capture the energy released. In a H_2-rich environment, life could use the reduction of N_2 to capture energy—in contrast to life on Earth which solely fixes nitrogen in an energy-requiring process. Energy capture would yield an excess of ammonia over that needed by life to build biomass, and so the excess would accumulate in the atmosphere as a Type I biosignature gas.

A catalyst is required to synthesize ammonia from hydrogen and nitrogen gas because the reaction in Equation (31) does not occur spontaneously at temperatures below 1300 K, at which temperature the formation of ammonia is strongly thermodynamically disfavored. On Earth, the industrial production of NH_3 by the above reaction is called the Haber process: an iron catalyst is used at high pressure (150–250 bar) to allow the reaction to happen at 575–825 K at which temperature the formation of ammonia is thermodynamically favored (Haber 1913). The Haber process is the principal industrial method for producing ammonia.[10] More efficient catalysts are known, which can catalyze the formation of ammonia from elemental nitrogen and hydrogen gases at 500 K and standard pressure (Yue et al. 2006; Avanier et al. 2007). Others catalyze the formation of ammonia from nitrogen gas and a proton (Yandulov & Schrock 2003; Shilov 2003; Weare et al. 2006) or from an activated nitrogen molecule and hydrogen gas (Nishibayashi et al. 1998), in water at room temperature and pressure. The final step of combining a room temperature nitrogen reduction catalyst with a room temperature hydrogen-splitting catalyst has not been achieved in the lab but is believed to be a realistic goal (Weare et al. 2006). Such a combined catalyst would make NH_3 from H_2 and N_2 and would generate energy (heat) from the reaction.

Life on Earth does not use the "Haber" reaction. This might be because the appropriate catalysts have not evolved. It might be because the rare environments in which H_2 is available provide other more easily accessible sources of energy (such as methanogenesis; Section 5.2). On Earth life inputs energy to break the N_2 triple bond, and the fixed nitrogen is a valuable resource representing an investment of energy and so is avidly taken up by other Earth life. Haber life using the Haber chemistry in an atmosphere with plenty of N_2 would produce generous amounts of NH_3, more than enough for the rest of life to use, enabling NH_3 to accumulate in the atmosphere as a biosignature gas.

To check the viability of NH_3 as a biosignature gas, we follow the steps listed in Section 3. For background, we consider a planet of Earth mass and size, a 290 K surface temperature and with a 1 bar atmosphere composed of 25% H_2 and 75% N_2 by volume, and including carbon species via a CO_2 emission flux from the planet's surface. NH_3 has significant opacity in the 10.3–10.8 μm band in a thermal emission spectrum. A mixing ratio of 0.1 ppm is radiatively significant for a 1 bar atmosphere in this band in a H_2–N_2 atmosphere (Figure 2) according to our detection metric (Section 4.3). We next determine the NH_3 surface source flux required for the gas to accumulate in the atmosphere to the 0.1 ppm concentration level. For this, we compute the photochemical equilibrium steady-state composition (results shown in Figure 3) with the ammonia surface source flux as a free parameter (Section 4.1). The dominant loss mechanism of NH_3 is due to photolysis (or reaction with OH; each process breaks the NH_3 bond) with some NH_3 eventually being converted to N_2. We adopt an NH_3 deposition velocity of 0 m s^{-1}, assuming that the surface is saturated in NH_3. (See below for a further discussion of deposition removal rate assumptions and related consequences.) The resulting NH_3 surface source flux is 5.0×10^{15} molecule m^{-2} s^{-1}. We note that this planet has a column-averaged mixing ratio of 0.4 ppm of NH_3, and to meet a surface temperature of 290 K, the semimajor axis would be 1.1 AU. We also point out that NH_3 concentrates mostly in the lower atmosphere, and decreases very rapidly with altitude above 15 km (Figure 3) because of the high-altitude destruction rates. To compute ΔG we used $T = 290$ K, and reactant and product concentrations at the surface in terms of partial pressures of $N_2 = 0.75$, $H_2 = 0.25$, and $NH_3 = 6.6 \times 10^{-7}$.

We next estimate the biomass surface density. Using the biomass equation (Equation (11)) with the NH_3 source flux of 5.0×10^{15} molecule m^{-2} s^{-1} (or 8.4×10^{-9} mole m^{-2} s^{-1}), $\Delta G =$ 75.0 kJ $mole^{-1}$ at 300 K, and $P_{m_e} = 7.0 \times 10^{-6}$ kJ g^{-1} s^{-1}, we find a biomass surface density of 8.9×10^{-2} g m^{-2}. We therefore consider the NH_3 production flux to be viable in our Haber World scenario. The global annual biogenic NH_3 surface emission in the Haber World would be about 6700 Tg yr^{-1}. This is much higher than Earth's natural NH_3 emission at 10 Tg yr^{-1} (Seinfeld & Pandis 2000). Comparing NH_3 production on the Haber World and on Earth, however, is not valid. We are postulating that production of NH_3 on the Haber World is a major source of metabolic energy for life. A better emission

[10] Fritz Haber and Carl Bosch were awarded the Nobel Prize for this chemistry in 1918, ironically, as the Haber process' principal deployment in the previous four years had been for making explosives for munitions, the application of chemistry that Alfred Nobel most wanted to discourage.

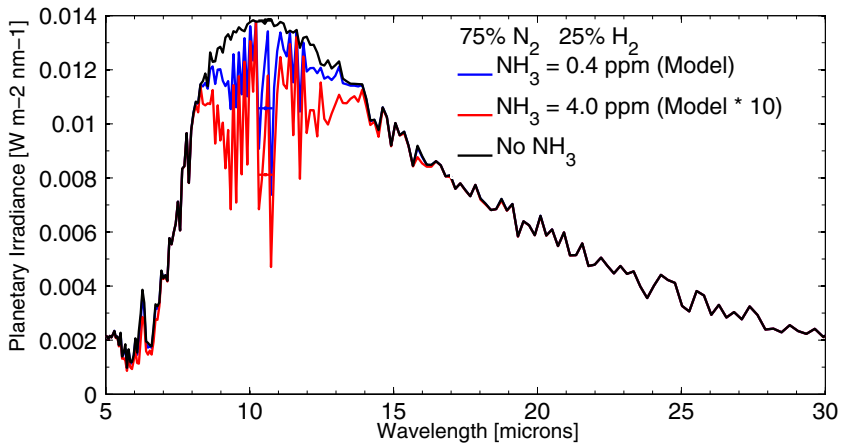

Figure 2. Synthetic thermal emission spectra for the "cold Haber World." The 1 bar atmosphere is composed of 75% N_2 and 25% H_2, with a 290 K surface temperature. NH_3 (that would be produced by life) is emitted from the surface. The spectrum in blue is computed from atmospheric composition calculated by the photochemistry model (the blue line in this figure corresponds directly to the composition shown in Figure 3). The spectra in red and black are computed with no NH_3 and 10 times more NH_3, respectively, for comparison. The spectra are computed at high spectral resolution and binned to a spectral resolution of 100. The horizontal bars show the broadband flux in the 10.3–10.8 μm band, most sensitive to the atmospheric NH_3 feature.

(A color version of this figure is available in the online journal.)

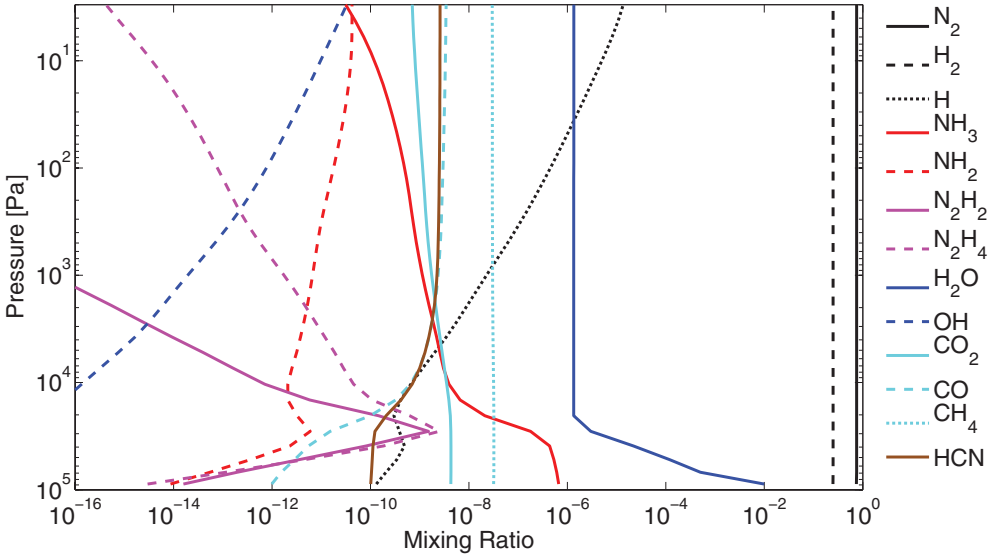

Figure 3. Mixing ratios for the atmosphere of the "cold Haber World." The 1 bar atmosphere is composed of 75% N_2 and 25% H_2, with a 290 K surface temperature. The simulated planet is an Earth-sized planet at 1.1 AU from a Sun-like star. The planet's surface is a net emitter of NH_3, with a surface source flux of 5×10^{15} molecule m^{-2} s^{-1} computed to match the 0.1 ppm concentration required by our detection metric. (Note that the present-day Earth's ammonia emission rate is 8×10^{13} molecule m^{-2} s^{-1}.) We also include CO_2 emission of 1×10^{14} molecule m^{-2} s^{-1} (one order of magnitude smaller than Earth's volcanic CO_2 emission). Our photochemistry model shows that NH_3 can accumulate to a mixing ratio of 0.4 ppm in the convective layer of the atmosphere while it is destroyed in the upper atmosphere layers.

(A color version of this figure is available in the online journal.)

rate comparison is to the biosignature gas O_2 from Earth's principal energy metabolism, photosynthesis. Earth's global oxygen flux is 500 times larger than the Haber World's NH_3 surface emission, at about 2×10^5 Tg yr^{-1} (Friend et al. 2009).

Deposition rates require more description, because on Earth deposition is the dominant atmospheric removal process for NH_3, yet we argue the deposition rates to play a minor role for NH_3 atmospheric removal on the Haber World. On Earth, ammonia is taken up avidly by life in soil and in water. On our proposed Haber World, life is a net producer of ammonia, not a net consumer, and so water (as raindrops or ocean) and soil would saturate with ammonia. Wet and dry deposition rates would therefore be limited to chemical consumption, the rates of which would depend on specifics of the surface chemistry. We therefore assume that the deposition rates are much less than atmospheric loss rates and this is considered in the photochemical calculation. A larger deposition rate implies a larger NH_3 emission flux and therefore a larger biomass to maintain the biosignature. When deposition is the dominant removal process, the relation between the source flux and the steady-state mixing ratio of NH_3 is linear. A Haber World with Earth-like NH_3 deposition rates (10^{-3} m s^{-1}) requires a NH_3 source flux of about 3.0×10^{17} molecule m^{-2} s^{-1} and a surface emission flux 100 times higher than the zero-deposition rate case. The biomass is also 100 times higher, and at $\Sigma_B \sim 9$ g m^{-2} is still a reasonable value.

The molecule HCN can be considered a bioindicator gas in the specific situation where HCN is detectable but its formation components, NH_3 and CH_4 (or any other dominant carbon source, such as CO or CO_2) are not. More specifically, in

a H_2-rich atmosphere, if NH_3 and CH_4 are emitted at comparable rates, HCN will be produced with little NH_3 and CH_4 remaining in the atmosphere above the convective layer (or above the first several scale heights from the surface; Hu et al. 2012). It can therefore be expected that if emissions of methane and ammonia are both elevated, the mixing ratio of HCN in the atmosphere can be as high as 1 ppmv and then become detectable via its prominent spectral feature at $\sim$3 μm. In other words, HCN can be an indicator of surface NH_3 emission, even if NH_3 itself is depleted and not detectable due to atmospheric photochemistry. The photochemical pathway of HCN under such conditions is described in detail in Hu et al. (2012). In general, in an atmosphere with enough NH_3 or N_2 and CH_4, the formation of HCN is inevitable in anoxic environments (Zahnle 1986). Also of potential interest, HCN is the second most common N-bearing species in the Haber World.

In terms of false positives for NH_3, the NH_3 biosignature gas concept is not changed in the massive atmosphere case with high surface pressure. As long as the surface conditions are suitable for liquid water, NH_3 will not be created by uncatalyzed chemical reactions. False positives may still exist such as chemical or biological breakdown of abiotic molecules. An additional false positive for NH_3 could be generated by non-life-compatible surface temperatures: at 820 K with surface iron, NH_3 could be generated by the conventional Haber process. These false positive statements hold for a rocky planet with a thin atmosphere; other cases such as planets with a massive atmosphere where NH_3 could be generated kinetically at extremely high pressures, or planets with icy interiors where NH_3 is outgassed during planetary evolution, have to be assessed on a case-by-case basis (see Seager et al. 2013).

In summary, we propose NH_3 as a biosignature gas on a planet with a N_2–H_2 composition. NH_3 should be photodissociated and therefore its presence would be indicative of biogenic production. We have nicknamed this planet "cold Haber World" because life would have to perform the Haber process chemistry using a highly efficient catalyst, low temperature to break both the N_2 triple bond and the H_2 bond, rather than the elevated temperature and relatively inefficient catalyst used in the industrial "hot" Haber process.

5.2. CH_4 on Terrestrial-like Exoplanets

We revisit methane as a biosignature gas on early Earth to estimate the biomass surface density required for primary producers to generate a remotely detectable CH_4 concentration.

CH_4 has long been considered a prime biosignature gas for Earth-like exoplanets (Hitchcock & Lovelock 1967) and especially for early Earth analogs (Des Marais et al. 2002). An early Earth analog prevalence of CH_4 theory is motivated by the early faint young Sun paradox. A few billion years ago, the Sun was 20%–30% fainter than today, specifically with 26% lower luminosity 4 Gyr ago, based on asteroseismology-constrained stellar evolution models (Bahcall et al. 2001). Yet, there is no evidence that Earth was frozen over during that time. A reduced greenhouse gas is a good, viable explanation for keeping Earth warmed despite the much cooler Sun (Sagan & Mullen 1972). The greenhouse gas CH_4 is a favored greenhouse gas explanation (Kiehl & Dickinson 1987; Haqq-Misra et al. 2008). Methane at 1000 times today's atmospheric concentration would have been sufficient to keep the Earth warm (i.e., concentrations of 1600 ppmv instead of 1.6 ppmv) (Pavlov et al. 2000; Haqq-Misra et al. 2008, and references therein). Moreover, accumulation of atmospheric CH_4 to levels much higher than Earth's would have been possible in the anoxic environment of early Earth. CH_4 could have accumulated to 1000 ppmv levels in the weakly reducing early Earth atmosphere because the CH_4 loss rate was so much smaller, owing to the lack of O_2. In more detail, the dominant removal rate of methane in an oxidized atmosphere is due to reaction with atmospheric OH. OH is produced via photochemistry, from both O_3 (itself a photochemical by-product of O_2) and H_2O (Seinfeld & Pandis 2000).

To consider the biomass required on any methanogenesis world, we must work with surface fluxes generated only by primary production methanogenesis. Overlooked or unstated for early Earth in past work is that most of Earth's biogenic methane production today is from fermentation of biomass. This biomass available for fermentation is almost entirely produced via photosynthesis. For an early Earth analog, before the rise of oxygenic photosynthesis, there is likely no large reservoir of biomass for fermentation. We note that on early Earth itself, there should have been a small reservoir of biomass, from, for example, anoxic photosynthesis. For exoplanets, we want to consider biologically produced methane from an ecosystem that uses methanogenesis as a primary energy source. In such a methanogenesis world, there would be biomass for fermentation, but the amount of methane produced by fermentation would be minor compared to the amount of methane produced from energy capture.

The methanogens of interest are those that convert H_2 and CO_2 to CH_4 in the process of extracting energy from the environment. These methanogens do not require biomass to feed upon and today live in anoxic environments, including hydrothermal vents at the deep sea floor, subterranean environments, and hot springs.

The methanogens of interest produce CH_4 by using carbon from CO_2 from inorganic sources,

$$H_2 + CO_2 \rightarrow CH_4 + H_2O. \quad (32)$$

At the deep-sea floor, H_2 is released from rocks by hot water emitted from hydrothermal vents (serpentinization). CO_2 is available dissolved in seawater. In other Earth environments, H_2 is also produced as a by-product of biological metabolism, and CO_2 is available as gas in air or dissolved in water. The metabolic by-products from methanogenesis are CH_4 and H_2O.

We now turn to the biomass estimate for CH_4 as the biosignature from a primary producing methanogenesis ecology on an early Earth analog exoplanet. We take early Earth (Earth-size, Earth-mass with a 1 bar atmosphere) to be an anoxic, N_2-dominated atmosphere with CO_2 mixing ratios of 1% and 20% (Ohmoto et al. 2004), the time period before the rise of oxygen (an Archaen atmosphere, 3.8–2.5 Gyr ago). For the planets to have surface temperatures of 290 K, they would be at 1.2 AU for the 1% CO_2 atmosphere and 1.3 AU for the 20% CO_2 atmosphere. Using our detection metric (Section 4.3), we find a detectable CH_4 mixing ratio to be 200 ppm in the 3.1–4 μm band. See Figure 4 for the chemical composition of the 1% CO_2 atmosphere.

Although we consider the effect of clouds on weakening the spectral features in the exoplanet spectrum, we do not treat formation of hydrocarbons that have more than two carbon atoms. The formation of hydrocarbons that have more than two carbon atoms should only have minor impact on our estimate of required biomass, because the most abundant hydrocarbons that have more than two carbon atoms, C_3H_8, has still five orders of magnitude lower mixing ratio at the steady state than C_2H_6 in N_2 atmospheres (Pavlov et al. 2001). The formation

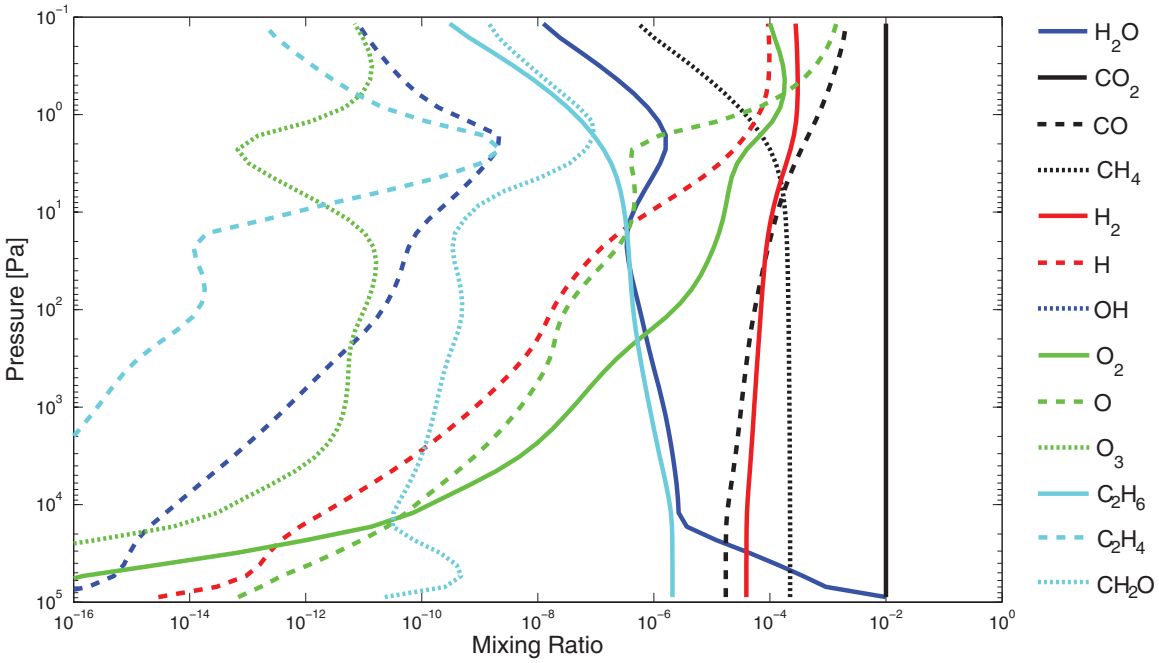

Figure 4. Atmospheric composition for the early Earth methanogenesis world. The 1 bar atmosphere is taken to be N_2-dominated with 1% CO_2. We take the planet's surface to be a net emitter of CH_4, with a surface flux of 7×10^{14} molecules m^{-2} s^{-1} computed to match the 200 ppm concentration required by our detection metric. Our photochemistry model shows that methane can accumulate to a mixing ratio of 220 ppm in the atmosphere and that the major photochemical product is H_2 having a mixing ratio of 40 ppm and CO having a mixing ratio of 18 ppm.

(A color version of this figure is available in the online journal.)

of hydrocarbon haze (commonly hydrocarbons with more than five carbon atoms), a point we do not address in this paper, may impact the energy budget of the planet and therefore the surface temperature (Haqq-Misra et al. 2008).

A CH_4 source flux of 7.0×10^{14} molecules m^{-2} s^{-1} (1.2×10^{-9} mole m^{-2} s^{-1}) and 5.0×10^{14} molecules m^{-2} s^{-1} (8.3×10^{-10} mole m^{-2} s^{-1}) is required to reach the 200 ppm CH_4 concentration in the 1% and 20% CO_2 atmospheres, respectively. To compute the ΔG value, we used the reactant and product molecule concentrations at the surface in terms of partial pressures as follows. For the CO_2 case of 0.01, we used $H_2 = 3.9 \times 10^{-5}$, $CH_4 = 2.2 \times 10^{-4}$, $H_2O = 0.01$, and this results in a $\Delta G = 47.4$ kJ $mole^{-1}$. In the CO_2 of 0.20 case, we used $H_2 = 1 \times 10^{-5}$, $CH_4 = 2.5 \times 10^{-4}$, and $H_2O = 0.01$, and this results in a $\Delta G = 41.2$ kJ $mole^{-1}$.

Using the above values, together with $P_{m_e} = 7.0 \times 10^{-6}$ kJ g^{-1} s^{-1} for the minimal maintenance energy rate for anaerobic microbes at 290 K, the biomass estimate is 7.8×10^{-3} g m^{-3} and 4.9×10^{-3} g m^{-3}, for the 1% and 20% CO_2 atmospheres, respectively, globally averaged values. This is a reasonable biomass as compared to terrestrial microbial biomass surface density values (Section 1.3). In this scenario, methanogenic organisms would dominate a biosphere where methanogenesis is the main energy source for life, just as on Earth photosynthetic organisms (including plants and water-based photosynthesizes) dominate the biosphere because photosynthesis is the dominant energy source for life.

For an early Earth analog "slime world," the critical question is whether H_2 would be a limiting input for methanogenesis on a planet with Earth-like atmospheric conditions (see Equation (32)). For the methanogenesis world, a global CH_4 flux of about 750 Tg yr^{-1} is required to reach the detectability threshold (this global CH_4 flux is the value corresponding to the CH_4 production rate calculated above). To investigate, we look at fluxes of hydrogen gas from Earth's hydrothermal systems and levels of hydrogen gas in hydrothermal fluids. Fluxes of hydrogen from hydrothermal systems on Earth can be as high as 1.8% of the total gases (see, e.g., Gerlach 1980; Le Guern et al. 1982; Taran et al. 1991). If this flux of H_2 is extrapolated to the global fluxes by comparison with fluxes of H_2S and SO_2 (Halmer et al. 2002), it would imply global H_2 fluxes of between 0.8 and 1.6 Tg yr^{-1}.[11] If all of the hydrogen were used in methanogenesis that would result in 3.2–6.4 Tg yr^{-1} methane.

If the H_2 needed to support the required rate of methanogenesis comes from volcanism alone—as in the case of modern Earth—a methanogenesis world with an Earth-like atmosphere, requires about 100 times more hydrogen flux outgassing than on present-day Earth. This high H_2 flux outgassing could be sustained by either a more reduced mantle (Holland 1984; Kasting et al. 1993), more serpentization, and/or more volcanism than on the present-day Earth.

The required large amounts of H_2 could be also produced from atmospheric photochemistry, in the absence of atmospheric oxygen, enabling a biochemical cycle to sustain surface methanogenesis. In our photochemistry code, atmospheric H_2 forms from photolysis of CH_4. The net accumulation of CH_4 results from the difference in production and loss of CH_4, being computed self-consistently with the appropriate mass balance. A form of this methanogenesis scenario was describe previously in Kharecha et al. (2005). In this biochemical cycle, a reasonable quantity of H_2 is required only at the onset of the evolution of methanogenesis.

We note that methane can reach high abundances through abiotic means especially if the mantle is reduced. More work is needed on false positives in the hope of finding a way to

[11] On Earth we do not see this flux of H_2 into the atmosphere because most H_2 is consumed at the point of emission by microorganisms in methanogenesis, reduction of sulfate, or by direct oxidation with atmospheric oxygen, so little escapes to the atmosphere.

distinguish biotic and abiotic methane, or at least to assign a probability to the chance of methane being biotic.

We finish the early Earth methanogenesis scenario with an emphasis on the deposition velocity as a loss rate. For CH_4, we have considered a zero deposition velocity, with the concept that a slime world covered in methanogens has a CH_4-saturated surface. We also assume that this world has few CH_4-consuming organisms compared to the CH_4-producing organisms. In other words, the rationale is that on a methane slime world, living organisms are net producers of CH_4 at the surface and would not destroy CH_4—the surface would likely be saturated in CH_4 making the deposition rate zero. On Earth, CH_4 deposited to the surface is rapidly oxidized by life to CO_2, so deposition is efficient, although only a minor contribution to the CH_4 loss rate. If we treat the N_2–CO_2 atmosphere with an Earth-like CH_4 deposition rate (for CH_4 on Earth typically 10^{-6} m s^{-1}), then CH_4 is prevented from accumulating to 200 ppm, but instead is at a lower concentration, at values of 15 ppm. A deposition velocity could be non-zero due to life other than the methanogens consuming CH_4; but see the discussion in Section 6.1.

To summarize this subsection, we have revisited methane as a biosignature gas on early Earth. We have found the biomass surface density needed to sustain a detectable CH_4 biosignature gas from primary production is reasonable at $\sim 5 \times 10^{-3}$ g m^{-2}. Although volcanism alone is unlikely to provide the amount of H_2 needed to sustain methanogenesis at the level required for CH_4 detection, an atmospheric photolysis of CH_4 can recycle the H_2 to provide sufficient flux.

5.3. Martian Atmospheric Methane

As a second case study, we apply our biomass model to the methane flux on Mars. CH_4 has been detected in the atmosphere of Mars with three independent instruments (Formisano et al. 2004; Krasnopolsky et al. 2004; Mumma et al. 2009). The Martian CH_4 detection is difficult to reconcile with present understanding of the planet and some believe the ground-based CH_4 detection may be a result of observational artifacts (see the references in the summary review by Atreya et al. 2011). The Martian CH_4 may be the result of geochemical outgassing or atmospheric photochemistry (Bar-Nun & Dimitrov 2006). A more intriguing, if speculative CH_4 source, is Martian life (Krasnopolsky et al. 2004). In this subsection, we show that the minimum required biomass density is plausible for the measured CH_4 fluxes.

Averaged CH_4 levels are 5–30 ppbv in the spring and summer mid-latitudes on Mars, depending on location, local time of day, and season (Formisano et al. 2004; Geminale et al. 2008, 2011; Mumma et al. 2009). There are pronounced local hot spots for methane concentration, hence presumably for CH_4 production. Different CH_4 observational studies, however, find hot spots in different regions (e.g., compare Mumma et al. 2009; Geminale et al. 2011), so we use global averages for our case study. The photochemical loss rate for the 5–30 ppb average level of CH_4 is $1–2 \times 10^9$ molecules m^{-2} s^{-1} (Wong et al. 2004; Krasnopolsky et al. 2004)

If Martian organisms were producing CH_4, they would be reducing atmospheric CO_2 with mantle-derived material, most plausibly H_2, so that the methane we observe would be the product of methanogenesis. We can calculate the free energy available from the reaction

$$4H_2 + CO_2 \rightarrow CH_4 + 2H_2O, \quad (33)$$

and hence estimate the biomass present in the soil that might account for the observed methane flux. The Gibbs free energy ΔG for methanogenesis under Martian daytime maximum temperature range (250–265 K) is calculated assuming the 15 ppb CH_4 surface flux, a likely surface hydrogen concentration of 15 ppm (Krasnopolsky & Feldman 2001), a CO_2 partial pressure of 0.95, and an H_2O partial pressure of 3×10^{-4}. ΔG is 85.2–77.5 kJ mole^{-1}. $P_{m_e} \simeq 7 \times 10^{-8}$ and $\simeq 5 \times 10^{-7}$ for temperatures at 250 K and 265 K, respectively. Combined with the surface flux above the CH_4 hot spots of the $1–2 \times 10^9$ molecules m^{-2} s^{-1} (Wong et al. 2004; Krasnopolsky et al. 2004), we find from Equation (11) surface biomass density of $\Sigma_B \simeq 10^{-6}$–10^{-7}. This a very small biomass surface density as compared to terrestrial biofilm values (Section 1.3), and hence the Martian CH_4 production by microbial life appears physically plausible.

The Martian surface is believed to be sterile, in part because the surface atmospheric pressure is incompatible with the existence of liquid water at any temperature and in part because the surface is unshielded from extremely destructive radiation from space (solar UV and X-rays and cosmic rays; Dartnell 2011). Water, if it exists near the surface, will be present as ice. Viking's finding of a complete lack of organic molecules in the top few centimeters of soil supports the sterility of the surface (Biemann et al. 1976, 1977). A few tens of centimeters of regolith would shield organisms from radiation (Pavlov et al. 2002). However, orbital radar suggests that water is frozen to a depth of several kilometers in most sites on Mars (reviewed in Kerr 2010), so Martian life must either be more deeply buried than current radar penetration, or be living in highly concentrated brines at depths of 1–3 km. The column-integrated density of $\sim 10^{-6}$–10^{-7} g m^{-2} of biomass would therefore be present not as surface life but living in rock interstices. This density is well below that of the density of such rock-dwelling microbial communities on Earth (Pedersen 1993 and references therein).

In summary, we have applied our biomass model to the putative methane detections on Mars. We found that if the CH_4 is produced by methanogenesis only a very small biomass surface density is required, $\Sigma_B \simeq 10^{-6}$–10^{-7} g m^{-2}. Martian methane could be generated by microorganisms living in subsurface rocks. Our model predicts that the amount of biomass needed to generate the proposed methane flux is plausible for a rock-based microbial community. By itself, a biomass surface density prediction does not rule out methanogenesis as the cause of the atmospheric CH_4.

5.4. H_2S: An Unlikely Biosignature Gas

The gas H_2S is generated by bacteria on Earth, and also by volcanism. The majority of Earth's H_2S emission is from life (Watts 2000). With our biosignature framework, we can calculate a consistent biosphere based on sulfur-metabolizing organisms and estimate how much biomass is required to generate a detectable amount of H_2S. Although detection of H_2S will be very difficult due to water vapor contamination of H_2S features, and just as seriously H_2S has a serious risk of false positive through volcanic production, the biomass estimate turns out to be reasonable.

H_2S would be very difficult to detect in a future exoplanet atmosphere spectrum, mostly because there are no spectral features that are not heavily contaminated by water vapor spectral features. In the UV, H_2S absorption features are mixed in with those of SO_2 and elemental sulfur,

both of which are likely to be present in the atmosphere with H_2S (http://www.atmosphere.mpg.de/enid/2295/; for specific UV cross sections see the references in Hu et al. 2012). At visible wavelengths, there are no prominent spectral features. In the infrared (IR), at 30–80 μm, a huge amount of H_2S would be needed to differentiate from water vapor spectral features. Even so, the H_2S features may cause a quasi-continuum absorption lowering the thermal emission flux below a reasonable detection threshold. There might be a way to detect H_2S in a spectrum that spans UV to IR: it might be plausible to detect total sulfur via UV spectral characteristics, infer from this a relative absence of SO_2, and then infer from an IR signature that there was a significant flux of H_2S (or DMS) from the ground. This is implausibly demanding of instrumentation, but not in theory impossible.

H_2S is commonly regarded as a poor biosignature gas because it is released by volcanoes. In general, we consider an atmospheric gas a potential biosignature gas if it is present in such large quantities that, in the context of other atmospheric gases, has no likely geological origin.

We nonetheless now turn to explore H_2S as a biosignature gas based on its biomass estimate. On a highly reduced planet, organisms could gain energy from reducing sulfate to H_2S, but in this environment H_2S would likely be the dominant volcanic sulfur gas as well. On an exoplanet with a more oxidized crust and atmosphere, we can imagine an ecosystem of sulfur disproportionators as the primary producers.

Microorganisms can disproportionate sulfur compounds of intermediate oxidation state, including thiosulfate, sulfite, and elemental sulfur, into H_2S and sulfate (Finster 2008). H_2S would be released as a biosignature gas. For example, the sulfite reducers include microorganisms in the genus Desulfovibrio and Desulfocapsa that obtain energy from the disproportionation of sulfite (Kramer & Cypionka 1989). The equation of the disproportion of sulfite in the ocean is

$$4HSO_3^- \rightarrow 3SO_4^{2-} + 2H^+ + H_2S. \quad (34)$$

Note that the accumulation of sulfite and sulfate in an ocean would make the ocean acidic, and at acidic pH levels, H_2S will exist in solution primarily as H_2S molecules, which will exchange readily with the atmosphere (unlike a neutral or basic ocean, where S(II) would exist as HS^- or S^{2-} which are not volatile).

To continue to explore H_2S as a biosignature gas, in our biomass estimate framework, we take an Earth-size, Earth-mass planet with a 1 bar exoplanet atmosphere composed almost entirely of N_2 with a minor H_2O concentration (like Earth above the cold trap but much drier below the cold trap) and a small amount of CO_2 (1 ppm), assuming volcanic emission. We consider detection at IR wavelengths, where absorption of H_2S might only be detected when the planet has a relatively dry troposphere (10^{-6} mixing ratio throughout the troposphere), meaning that there will be reduced contamination of H_2S spectral features by water vapor. Even for an extremely high H_2S emission (3000 times Earth's volcanic emission) on a desiccated planet, we have estimated an H_2S concentration of 10 ppm for detection via thermal emission in the 45–55 μm range according to our detection metric (Section 4.3). The H_2S surface flux required is 3000 times Earth's volcanic emission (10^{17} molecules m^{-2} s^{-1}). The SO_2 surface flux (used by the sulfur disproportionators) is scaled up accordingly (two times the H_2S surface flux). To compute the ΔG value, we used the reactant and product molecule concentrations at the surface in terms of partial pressures as follows: $SO_2 = 2.9 \times 10^{-7}$ and $H_2S = 9.4 \times 10^{-6}$, and we assumed the ocean was saturated with sulfate (1.1 mole liter^{-1}) with an ocean pH of 3 (i.e., 10^{-3} mole). This results in a $\Delta G = 71.3$ kJ mole^{-1}.

To summarize, using Equation (11) and the values $P_{m_e} = 7.04 \times 10^{-6}$ kJ g^{-1} s^{-1} at 290 K, $F_{\rm source} = 3.0 \times 10^{17}$ molecule m^{-2} s^{-1} (or 5.0×10^{-7} mole m^{-2} s^{-1}), and $\Delta G = -71.3$ kJ mol^{-1}, we find a surface biomass density of about 5.1 g m^{-2}. The total flux produced on an Earth-sized exoplanet would be 4.0×10^5 Tg yr^{-1}. This total flux is very high, on the order of 10^5 times more than H_2S produced on Earth, and similar to the benchmark values for primary production of carbon on Earth.

A further challenge with H_2S as a biosignature (or even as a geosignature) has to do with atmospheric photochemistry. As soon as H_2S (or SO_2) is released into the atmosphere at an amount greater than 10–100 times Earth's current H_2S or SO_2 surface flux, a blanket of aerosols or condensates form. These aerosols or condensates are present at optically thick amounts, potentially masking any H_2S or SO_2 spectral features, depending on the particle size distribution.

As a side note we explain why we consider sulfur dioxide, SO_2, is a failed potential biosignature gas, even though it is a gas produced by life. SO_2 as a Type I biosignature would result from the oxidation of sulfur or sulfides, via the reaction

$$S_2^- + 3[O] + 2H^+ \rightarrow SO_2 + H_2O \quad (35)$$

$$S + 2[O] \rightarrow SO_2, \quad (36)$$

where [O] represents an oxidizing agent, such as Fe^{3+} or O_2. The resulting SO_2 would almost certainly be dissolved in water as sulfite; in an oxidized environment further energy would be generated from oxidizing sulfite to sulfate

$$SO_3^{2-} + [O] \rightarrow SO_4^{2-}. \quad (37)$$

So, if the environment is sufficiently oxidizing to allow energy generation from sulfide oxidation, the end product is likely to be sulfate, not SO_2. Furthermore, because SO_2 is geologically generated, it would be hard to distinguish from biogenic SO_2. If there are oxidants available for life (i.e., there are oxidants available for life to use to oxidize sulfides for energy), then the crust and upper mantle will also be oxidized, and SO_2 will be a major volcanic gas.

In summary, H_2S is a potential biosignature gas as seen from the view of a biomass estimate, in a reduced atmosphere where H_2S can accumulate. In general, H_2S is ruled out as detectable or identifiable as a biosignature gas because of its weak or H_2O-contaminated spectral features and because of geological false positives.

5.5. CH_3Cl on an Earth or Early Earth Type Atmosphere

We now turn to the Type III biosignature gases, using methyl chloride CH_3Cl as the example. On Earth, CH_3Cl is thought to generated mostly by land soils (by plants; Keppler et al. 2005), changed from an earlier view that phytoplankton in the open ocean contributed most of Earth's CH_3Cl. On Earth, CH_3Cl has a global production rate of between 2 and 12 Tg yr^{-1} (see Table 1, and references therein). Averaged over Earth's land mass, the CH_3Cl translates into a source flux of 3.2×10^{-12} mole m^{-2} s^{-1}. This value of source flux does not produce a detectable biosignature gas in the "Earth as an exoplanet spectrum," where CH_3Cl has a mixing ratio of 1 ppb.

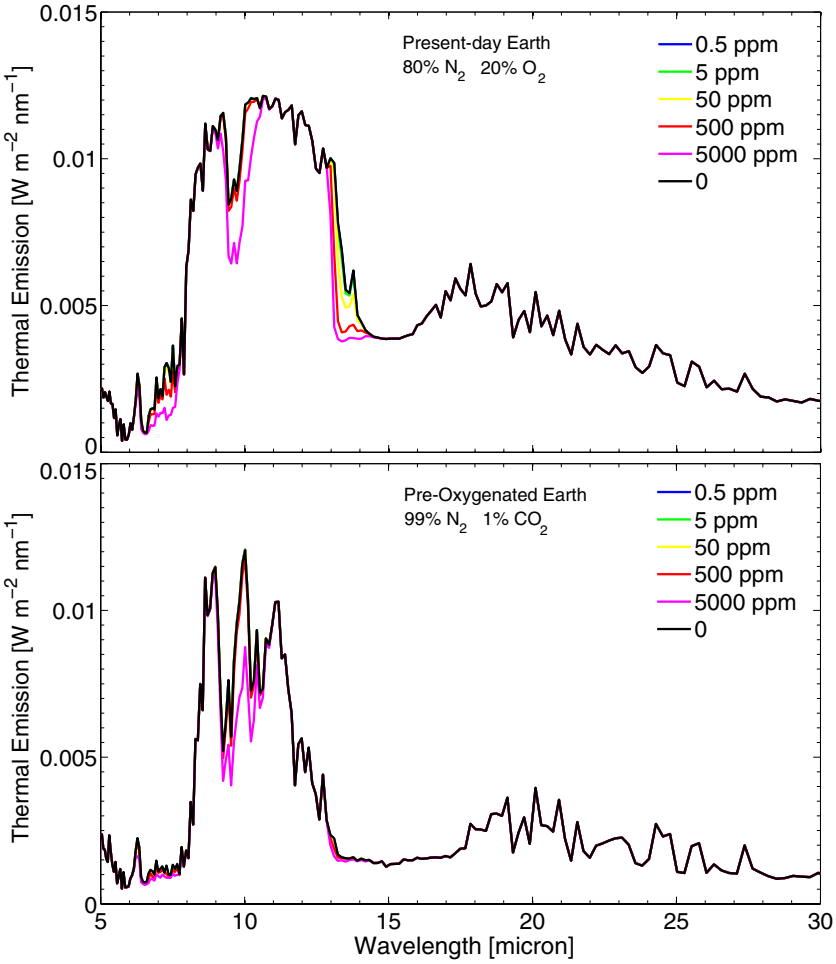

Figure 5. Synthetic spectra of terrestrial exoplanets with various levels of CH_3Cl. Top panel: present-day Earth's atmosphere with N_2, O_2, H_2O, CO_2, and other photochemical derivatives. Bottom panel: pre-oxygenated Earth's atmosphere with N_2, CO_2, H_2O, CH_4, and other photochemical derivatives. The spectra are computed at high spectral resolution and binned to a spectral resolution of 100. The main point of this figure is how challenging it would be to detect CH_3Cl.

(A color version of this figure is available in the online journal.)

For an Earth-like atmosphere around a low-UV quiet M dwarf, CH_3Cl can accumulate up to 1 ppm (Segura et al. 2005).

For an Earth-like exoplanet atmosphere spectrum, CH_3Cl is a difficult biosignature gas to detect because of its overlap with other spectral features, notably O_3 or CO_2. As reported in Segura et al. (2005), the CH_3Cl spectral feature at 9.3–10.3 μm coincides with the O_3 9.6 μm band, and would be difficult to identify, necessitating detection of CH_3Cl features at 13–15 μm or a weaker feature near 7 μm. Under the conditions of a UV-quiet M star with low OH concentration, Segura et al. (2005) have shown that CH_3Cl in an Earth-like atmosphere orbiting a quiet M dwarf can accumulate to 1 ppm. In an N_2 atmosphere with little CO_2, CH_3Cl would be easier to detect, but still difficult owing to even a tiny amount of atmospheric CO_2.

With our framework for biomass estimates, we ask the question, "what biomass surface density of CH_3Cl-producing life is required to generate a detectable CH_3Cl biosignature gas?" We answer the question for present-day Earth and for early-Earth conditions before the rise of atmospheric O_2. We take a planet of Earth's size and mass with an Earth-mass atmosphere. The temperature profiles are self-consistently computed with photochemistry, and the semimajor axis of the planet is adjusted so that the surface temperature is kept at about 300 K.

For a planet with the present-day Earth atmosphere concentration, our detection metric (Section 4.3) finds a 20 ppm mixing ratio at 13–14 μm on the short-wavelength wing of the 15 μm CO_2 band (note that in Earth's atmosphere, the CO_2 concentration is low enough not to fully saturate the 15 μm wing). The concentration of 20 ppm is 20,000 times more than Earth's current atmospheric concentration of CH_3Cl, a value of 0.001 ppm. See Figure 5.

The Type III biomass equation scales linearly (Equation (21)), so for all other atmospheric conditions being equal to the present-day Earth, the biomass must therefore be 20,000 times higher than the present day. By adopting the scaling relationship, we also assume that the 20 ppm concentration of CH_3Cl is not enough to feed back on the dominant destructing molecule [OH] concentration or to significantly effect the temperature–pressure profile.

Is it reasonable to imagine a world with a planet biomass surface density of CH_3Cl-generating life 20,000 times higher than on Earth? If the conventional view that CH_3Cl is produced overwhelmingly by oceanic plankton is adopted, then densities of tens of kilograms of phytoplankton per m^{-2} in the oceans would be required. If the more recent view that land plants are a major source of CH_3Cl, then a 20,000-fold increase in biomass requires all the planet's land be covered with plants at a density not even achieved in the most intensively farmed land in the most favorable conditions. Neither seem plausible. We can only escape from this conundrum if we

assume that a much larger fraction of organisms on an exoplanet produce CH_3Cl, or they produce it at a much higher rate than organisms on Earth. We have no reason for making such assumptions.

We now turn back to Earth's past, prior to the oxidation of Earth's atmosphere, with solar-like EUV conditions, where the CO_2 concentration was thought to be as high as 1% to 20% by volume (Ohmoto et al. 2004). In an atmosphere with so much CO_2, CH_3Cl is much harder to detect than on present-day Earth because of overlap with the 15 μm CO_2 feature, the CH_3Cl feature at 10 μm must be considered. A CH_3Cl concentration of 1000 ppm would be needed (and barely detectable according to our detection metric), for either the 1% or 20% CO_2 atmosphere, requiring a surface biosignature gas source flux of 3.5×10^{19} m^{-2} s^{-1} (or 5.8×10^{-5} mole m^{-2} s^{-1}). Although our photochemistry code does not yet self-consistently treat halogentated compounds, we computed this surface source flux by considering the loss rates: the source flux, $F_{\rm source}$, is the production rate P integrated over an atmosphere column, and P is related to the loss rate L, (recall Section 4.1)

$$F_{\rm source} = \int_z P = \int_z [CH_3Cl](z) L(z) = \int_z [CH_3Cl](z)[OH](z) K_{CH_3Cl,OH}(z), \quad (38)$$

where [OH] is the main reactive molecule that destroys CH_3Cl. The loss rate scales linearly with [OH], as long as the concentration of CH_3Cl does not affect [OH]. For values of reaction rate K, see Table 7.

The estimate of the surface biomass density required for a surface source flux of 3.5×10^{19} molecules m^{-2} s^{-1} can be found using the estimate for the Type III biosignature gases (Equation (21)). For CH_3Cl, we find $\Sigma_B = 9.4 \times 10^5$ g m^{-2} higher than any reasonable biomass surface density. The uncertainties in the Type III biomass estimate, however, should be considered.

To summarize this subsection, Type III biosignature gases are not produced in large quantities on Earth because they are specialized chemicals, each produced by a small number of species. Furthermore, collisional destruction by OH is rapid. Type III biosignature gases have shown to be detectable in low-UV environments, which as a consequence have less OH. We have shown that in order to reach detectable levels on present-day Earth, we can scale up the biomass estimates based on the concentration of the atmospheric gas required for detection, although in the case of CH_3Cl this results in an implausible biomass surface density.

6. DISCUSSION

6.1. On the Order of Magnitude Nature of the Biomass Estimates

The biomass estimates are limited to an order of magnitude for Type I biosignatures, and about two orders of magnitude for Type III biosignature gases.

Estimates of the Type I biomass are dependent on P_{m_e} whose constants are known to 40% 1σ (Tijhuis et al. 1993), and P_{m_e} is very sensitively dependent on temperature, due to an exponential term (Equation (15)). Small changes in surface temperature estimates can have very large effects on P_{m_e}. Of equal importance is that chemical reaction rates also exponentially increase with temperature.[12] For the same change in temperature, the rate of destruction (and hence production) of a gas $F_{\rm source}$, and the minimal maintenance energy rate P_{m_e} have opposite, although not necessarily balanced, effects on our estimate of biomass, via the Type I biomass equation (11). The effect of temperature uncertainty needs to be further investigated. A more minor contribution to the inaccuracy of Type I biosignature gases is that the energy released in a reaction (captured ΔG) varies with pH, and reactant and product concentrations, none of which are known for exoplanet environments.

The Type III biomass estimate is uncertain because it is not constrained by thermodynamics. The accuracy-limiting assumption for the Type III biomass estimate is that exoplanet biosignature gas production rates are the same as those found in Earth's lab-based maximum production rates.

Unlike applied physics, we do not know everything about biology, we do not know everything about Earth, and we do not know everything about atmospheric chemistry. In other words, the model is not 100% accurate and we must live with uncertainty in the biomass estimates. The point is that the biomass estimate should be used to answer the question, "Is the proposed biosignature gas plausible?" and not for any kind of precise prediction of biomass surface densities.

6.2. On the Possible Terracentricity of the Biomass Estimates

A question arises as to the terracentricity of the biomass estimates, and whether or not we have interchanged the conventionally used Earth-based surface biofluxes with an Earth-based biomass model estimate.

For the Type I biosignature gases we argue no, because thermodynamics is universal. The Type I biosignature biomass model uses a prefactor A and an activation energy E_A for the minimum maintenance energy rate P_{m_e} equation. These parameters are lab-measured values for Earth-based microbes. A critical question is to what extent are A and E_A specific to Earth life. A simple argument is that the particular repair mechanisms and molecular turnover involved in maintaining an organism are specific to Earth life, which is very unlikely to be exactly replicated on other worlds. There are stronger arguments, however, that the energy rate is more broadly applicable: P_{m_e} follows Arrhenius' law, we think because the rate of molecular component damage (and hence repair rate) is no different than other chemical reactions—well described by an Arrhenius equation. E_A, the activation energy of a reaction, represents the energy needed to break chemical bonds during the chemical reaction. In uncatalyzed reactions, E_A comes from the thermal energy of the two reacting molecules, which itself follows from the Boltzmann velocity distribution. The probability that any two colliding molecules will have a combined energy greater than E_A is $\exp[-E_A/RT]$. The parameter A is an efficiency factor that takes into account that molecules have to be correctly oriented in order to react. Thus, the basic physics of the Arrhenius equation is general to all chemistry.

The argument for applying the Arrhenius equation to calculating P_{m_e} starts with the point that terrestrial life is composed of many of the possible structures in CHON chemistry. The principal way that random chemical attack breaks those molecules down is through hydrolysis (attack by water) or oxidation (attack

[12] Chemical reaction rates often follow exponentials, especially reactions involving stable species, of the form $R \sim C \exp(T/k)$, where R is the reaction rate, C is a constant, T is temperature, and k is a constant.

by oxygen) if oxygen is present. The A and E_A terms in the equation for P_{m_e} represent those relevant to the breakage of the most fragile of metabolites (as more stable molecules will not need to be repaired). Although the specific chemicals in non-terrestrial metabolism could be quite different from those on Earth, the nature of the chemical bonds will be similar. In particular, non-terrestrial biochemistry will be made up of chemicals that are moderately stable at ambient temperature and pressure, but not too stable. Thus, the overall distribution of molecular stability in a non-terrestrial metabolism is likely to be similar to that in terrestrial metabolism, even if the chemical specifics differ. As a consequence, it is reasonable to propose that the rate of breakdown of those metabolites, and the rate at which energy is needed to repair them (i.e., P_{m_e}) will be of a similar order of magnitude as the rate of breakdown and energy requirement seen on Earth. Therefore, A and E_A are likely to be based on chemical principles and therefore similar to those calculated for Earth.

Turning to the terracentricity of the production rates for Type III biosignature gases, they are derived from lab measurements of each organism and are likely to be specific to those organisms. The rates may, however, be plausible indications of the Type III fluxes to be expected from non-terrestrial life because the gas production represents investment of energy and mass for a specialized biochemical function. The maximum flux rates used here represent the maximum investment that organisms make in these Type III gases, given essentially unlimited energy and nutrient resources in a lab environment. We speculate that it is unlikely that non-terrestrial life would be more wasteful of resources through making any Type III biosignature gas at rates orders of magnitude greater than those used in this study.

The biomass surface density limits we use as a reference point are based on Earth data, and so are terracentric. We believe that adopting Earth values is an acceptable approximation in our model, as what limits Earth life in environments with abundant nutrition is the physics of mass transfer, not the specifics of how Earth life evolved. This, however, should be validated by future research.

We do not argue the biosignature biomass model estimates are accurate; rather we emphasize the goal of the biomass model estimate is the nature of the order of magnitude for a first-order assessment of the plausibility of a given biosignature gas candidate.

6.3. Biomass Estimates in the Context of an Ecology

A serious criticism against the biomass estimate is lack of an ecology context. An ecology will contain organisms that consume gases as well as produce them. Hence, the concern is that potential biosignature gases will be destroyed by life in the same ecosystem, rendering the biomass estimates invalid. Indeed, the biomass estimate must be a minimum biomass estimate because there is no guarantee that biosignature gas flux ($F_{\rm source}$) is not being consumed by other organisms.

The biomass estimate model is intended as a check on the plausibility of a specific gas as a biosignature gas. It is not intended to be a prediction of the ecology of another world. If the biomass estimate is low, then we have confirmed that the gas is plausible as a biosignature, given the caveats presented in Sections 6.1 and 6.2 and discussed throughout this paper. In this low biomass estimate case, even if the planetary ecology has a mix of gas-producing and gas-consuming organisms, a net production of the gas from a moderate biomass is quite plausible. If the biomass estimate is too high, the gas is not a plausible biosignature gas in any ecology. For the intermediate case where a large but not unreasonable biomass is needed to generate a detectable biosignature, the decision on whether the gas is a plausible biosignature is more complicated, and will depend on the context: geochemistry, surface conditions, atmospheric composition, and other factors.

In the future when we have spectra with candidate biosignature gas detections, in most cases we will assign a probability and not a certainty to a biosignature gas candidate. The biomass estimate, in the context of an ecology, will be just one of the input factors to the probability assessment. We give an example here to sketch out other factors to consider, which also bear weight on the ecology. The example is the question, how would we interpret the detection of 500 ppm CH_3Cl in the atmosphere of an anoxic, Earth-like planet (well above the detectable amount according to our detection metric and assumed future telescope capabilities)? Our biomass model predicts that we would need a highly implausible surface biomass density to generate such an atmospheric concentration through metabolism. Volcanic chemistry on Earth produces traces of methyl chloride, but only as a tiny fraction of emitted gases, making a volcanic source seems also highly improbable. Conceivably, the CH_3Cl could be an industrial waste gas from a technological civilization, but in the absence of other signs of civilization this is also improbable. In this abstract sense, the conundrum of the intermediate biomass estimate has no solution, but the plausibility of a biosignature gas is still addressable through Bayesian statistics in principle, if the prior probabilities of the different assumptions about geochemical sources, biological sources, or technological sources can be estimated. Our biomass model provides a numerical approach to quantifying the assumptions made concerning the potential biological production of a biosignature gas. Further work will integrate this into a model of our confidence that the detection of the gas represents a detection of life.

6.4. Massive Atmospheres and the Biomass Estimates

In an atmosphere more massive than Earth's 1 bar atmosphere, the biomass surface density estimates could be different, depending on the biosignature gas loss rate mechanism. In an atmosphere where the photochemical loss rates dominate, the biosignature source flux and hence biomass is the same as for a less-massive atmosphere. In an atmosphere where the deposition rate is the dominant loss mechanism, the biosignature source flux and hence biomass surface density will scale linearly with planetary atmosphere mass. These conclusions are under the caveat that the surface pressure and temperature do not cause unusual chemistry (e.g., supercritical fluid or high chemical kinetic rates).

The biosignature source flux (i.e., production rate) is balanced by the loss rate, as described in Equation (22). Photochemical removal is only effective at and above the mbar pressure level in the atmosphere, because the UV radiation typically penetrates only down to the mbar level. The loss rate is therefore unaffected by how much atmosphere there is below the mbar pressure level: the mbar level can be "sitting on top of" a small atmosphere or a very large one. Hence, the loss rate is the same (all other factors being equal) regardless of the total mass of the atmosphere. The loss rate is balanced by the source flux and hence the source flux needed to maintain a given concentration of gas in an atmosphere is unaffected by the mass of the atmosphere (assuming that there is no new, non-photochemical loss of gas at much higher pressures). Thus, against loss from photochemistry, the surface

biomass density required to maintain a given gas concentration is the same regardless of atmospheric mass for any planet of a given surface area.

Loss by deposition, in contrast to loss by photochemical removal, occurs at the planetary surface. The loss rate at the surface is proportional to the number density of the biosignature gas at the surface (see Equation (28)) The number density of any well-mixed species scales as the surface pressure for an ideal gas atmosphere in hydrostatic equilibrium. We can estimate the surface gas concentration $n_{\rm ref}$ by considering a uniformly mixed atmosphere and integrating over a vertical atmosphere column under hydrostatic equilibrium,

$$\int_{p_0}^{p_{\rm ref}} dp = -\int_0^{z_{\rm ref}} g\rho dz, \tag{39}$$

where p is pressure and g is surface gravity. Here, we integrate from $p = 0$, $z = 0$ at the top of the atmosphere down to a reference pressure $p_{\rm ref}$ at a reference altitude. Integrating the above equation, we have

$$p_{\rm ref} = g m_{\rm atm}, \tag{40}$$

where $m_{\rm atm}$ is the atmospheric mass in a vertical column of 1 m^2 cross-sectional area. We can therefore define $n_{\rm atm}$ by rewriting the column-integrated mass of the atmosphere in terms of number density and the mean molecular mass of the atmosphere $\mu_{\rm atm} m_H$ (where μ is the mean molecular weight and $m_{\rm H}$ is the mass of the hydrogen atom,

$$X_i n_{\rm ref} = X_i \frac{p_{\rm ref}}{kT} = \frac{g m_{\rm atm}}{kT}, \tag{41}$$

where X_i is the mixing ratio of the gas under consideration.

We can now explain why, when surface deposition is the dominant gas loss mechanism, a larger biosignature surface density is required as an atmosphere mass scales up, even for a fixed atmospheric gas concentration. We see from Equation (41) that the gas number density at the surface scales with the surface pressure $p_{\rm ref}$. The deposition velocity scales with the number density and hence surface pressure. With a higher loss rate that scales linearly with surface pressure, a higher source flux (production rate) is required to balance the loss rate. Because biomass scales linearly with source flux, a higher biomass surface density is required.

6.5. False Positives

Type I biosignature gases are fraught with geologically produced false positives because geological processes have the same chemicals to work with as life does. The redox reaction chemical energy gradients exploited by life are thermodynamically favorable but kinetically inhibited. Enzymes are used by life to accelerate the reaction. We can be sure that a chemical reaction that is kinetically inhibited in one environment on Earth could proceed spontaneously somewhere else on the planet (in an environment with a favorable temperature, pressure, and reactant concentrations). Hence, Type I biosignature gases will almost always have a possible geological origin.

Typically astronomers assume that the biosignature gas must be produced in high enough quantities that it could not be confused with a geophysical false positive. But how high of a surface flux could be produced geologically? We plan to model the maximal geofluxes possible for planets of different characteristics (Stamenkovic & Seager, in preparation), with the end goal of assigning a probability to the dominant Type I biosignature gases (H_2S, CH_4, CO, CO_2, N_2O, NO, and NO_2) for being produced as biofluxes versus geofluxes. More progress might also be made with biogeochemical cycles and the whole atmosphere context via other atmospheric diagnostics.

False positives for O_2, the most obvious Type II biosignature gas in an oxidizing environment, are limited and can most likely be identified by other atmospheric diagnostics. For example, photodissociation of water vapor in a runaway greenhouse with H escaping to space could lead up to detectable O_2 levels. This situation could be identified by an atmosphere heavily saturated with water vapor. O_2 could also accumulate in a dry, CO_2-rich planet with weak geochemical sinks for O_2, a case which could be identified via weak H_2O features (Selsis et al. 2002; Segura et al. 2007).

Type III biosignature gases, in contrast to Type I biosignature gases, are less likely to have false positives. Type III biosignature gases are chemicals produced by life for reasons other than energy capture and are not usually naturally existing in the environment. As by-product gases of highly specialized physiological processes, the Type III biosignature gases tend to be larger or more complex molecules than Type I biosignature gases, and are not usually replicated by non-biological processes. In general, the more complicated a molecule is (i.e., the more atoms it has) and the further from fully oxidized or reduced the molecule is, the less are produced by geological sources as compared to more simple molecules. For example, volcanoes produce large quantities of CO_2, somewhat smaller amounts of CH_4, small amounts of OCS, trace amounts of CH_3SH, and none of isoprene. The downside to Type III biosignatures is that because they are usually such specialized compounds they typically are produced in small quantities that do not accumulate to levels detectable by remote sensing.

For Type III biosignature gases, we should therefore depart from requiring huge concentrations in the atmosphere. But, as we have seen, detectable atmospheric concentrations are almost by definition high concentration.

Light isotopes are used to identify biologically produced molecules on Earth. For exoplanets, no planned telescope will allow molecular isotopes to be observationally distinguished from one another. In the distant future when isotopic ratios of molecules are observable, care has to be taken to understand the isotopic distribution of all key molecules in the environment. In particular, the isotopic ratios of the input gases must be different than the biologically output gases. The isotopic ratios of both the input and output gases need to be inventoried, because exoplanets may have varying natural distributions of isotopic ratios not seen on Earth.

6.6. Aerosols and Hazes

The view in biosignature gas studies is to find a biosignature gas that exists in concentrations of orders of magnitude above the naturally occurring values. This picture may supercede the goal to find biosignature gases that are out of redox equilibrium (such as O_2 and CH_4) because while both might exist they might not both be in high enough quantities to be detectable remotely.

For a biosignature gas produced orders of magnitude higher than natural values, how much is too much? We have seen from our H_2S study (Section 5.4) that when H_2S is emitted from the surface at an amount greater than 10–100 times Earth's current H_2S or SO_2 surface flux, a blanket of aerosols or condensates form (Hu et al. 2013). These aerosols or condensates are present

at optically thick amounts, masking any H_2S or SO_2 spectral features. The particle size partially dictates the optical properties of the aerosols, and hence which wavelengths the spectral features will be washed out.

Aerosol formation by CH_4 photolysis in N_2–CO_2 atmospheres are expected to be significant when methane reaches 5000 ppmv (Haqq-Misra et al. 2008). There are two effects if aerosol formation is significant. First, aerosols may be a net loss for CH_4, leading to a decreasing marginal gain in atmospheric CH_4 concentration for increasing CH_4 emission. Second, aerosols may impede CH_4 detection. As an aside we point out a basic assumption in the haze formation model used by Haqq-Misra et al. (2008) that could be improved upon a treatment of all hydrocarbons higher than C_4 as solid particles when they might be in the gas phase makes hazes easier to form.

NH_3 emission itself does not lead to aerosol formation, as NH_3 is readily converted to N_2 by photolysis.

The situation for DMS is virtually the same as H_2S and SO_2. Sulfur in the terrestrial atmosphere is likely to end up as aerosols (S_8 and H_2SO_4, for H_2S and SO_2, respectively). The reason is that S_8 and H_2SO_4 are relatively easy to form from sulfur gas compounds, and they have relatively low vapor pressures enabling aerosol formation at Earth atmospheric temperatures (see Seinfeld & Pandis 2000).

6.7. Subsurface Life

If the surface of a planet is not habitable, could the subsurface harbor life? On Earth, there is substantial subsurface life, but its effect on the atmosphere is limited. On Earth, surface life will likely use any product of subsurface life as a food source, generating the characteristic biosignature gas of the surface life. Thus, H_2S or CH_4 emitted by subsurface life on Earth is (largely) oxidized at the surface, and so does not accumulate in the atmosphere.

If the surface is not habitable, however, then any subsurface biological activity will eventually affect the surface, just as surface biology on Earth eventually oxidized the stratosphere. In the absence of surface life, subsurface life biosignature gases will diffuse to the surface and then escape. (The methane on Mars may be an example of this.) If Mars had surface life, then that surface life would "eat" all the methane, and none would accumulate in the atmosphere. Thus, our model is applicable to the biomass of subsurface life as well as surface life, with the caveat that we do not know what a plausible upper boundary on the density of subsurface life is.

There remains the problem that subsurface life will generate gases that are just absorbed by the surrounding material (rock, ice, or water). If life is too deep (as life in the internal oceans of the Gallilean moons would be, if there is any) then biosignature gases would take geological time to reach the surface, and would be chemically transformed by the interposed geology (rocky or icy) in the process. In other words, if life is deep, the rock will only saturate on geological timescales, and over that time any biosignature will be chemically converted to other substances. If life is subsurface but shallow, rocks will become saturated with biosignature gases in a short timescale and the biosignature may then be outgassed to the atmosphere.

6.8. Life on Titan: Ruled Out by Biomass Calculations?

It has been speculated that anomalies in the atmosphere of Titan could be signs of surface life. With substantial caveats, we can apply the biomass model to test the plausibility of Titanian life. Acetylene is not detected on the surface of Titan, as reported by Clark et al. (2010), although some models suggest that acetylene should be more abundant on the surface than benzene, which was detected. There is an apparent deficit of acetylene on Titan's surface, because acetylene was detected in Titan's atmosphere. Strobel (2010) modeled the atmosphere of Titan, and predicted a tropospheric deficit of H_2 in Titan's atmosphere, compared to stratospheric levels, implying a downward flux of H_2 of the order of 2×10^{14} m^{-2} s^{-1}. Several authors have speculated this is a sign of life on Titan (see, e.g., Norman 2011; Seager et al. 2012),[13] deriving energy from either of the following reactions:

$$C_2H_2 + 2H_2 \rightarrow C_2H_6 \quad \Delta G_0 = -242 \text{ kJ mole}^{-1} \quad (42)$$

$$C_2H_2 + 3H_2 \rightarrow 2CH_4 \quad \Delta G_0 = -375 \text{ kJ mole}^{-1}. \quad (43)$$

We can test the hypothesis that the acetylene deficit is a biosignature gas using the Type I biomass model. Life on Titan could live on the surface, using liquid methane as a solvent (Bains 2004; McKay & Smith 2005), or near the surface, or in the deep interior using water as a solvent. Life in liquid methane/ethane at ~100 K must have radically different chemistry from terrestrial life; it is almost inevitable that the biomass model in Equation (11) will not be valid for such different biochemistry. Specifically, we might expect the constant A term in the minimal maintenance energy rate equation (15) to be lower for liquid methane life. The major source of damage for terrestrial biomolecules is attack by water, which will be much slower when the molecules are not dissolved in water. While we have no idea how much smaller A should be, we can, however, still attempt to apply Equation (11) to predict the minimum biomass necessary to generate a biosignature gas. If on Titan the P_{m_e} constant A is smaller than on Earth, then from Equation (15), the minimal maintenance energy rate P_{m_e} will be smaller (at a given temperature), and so from Equation (11) our biomass estimate will be larger.

If hydrogen and acetylene are being consumed by water-based life on Titan today, then that life must be near the surface. Water near the surface would freeze to a eutectic of whatever solutes are present in the internal ocean—as these are unknown, we have assumed a water/ammonia eutectic with a freezing point of 176 K (Leliwa-Kopystyński et al. 2002). The deeply buried "internal ocean" is likely to be warmer, but is too deeply buried to account for a high surface flux of hydrogen (Fortes 2012); however, we include a calculation for a saturated freezing brine at 252 K for comparison.

The flux of H_2 downward is proposed to be 2×10^{14} m^{-2} s^{-1} $= 3.3 \times 10^{-10}$ mole m^{-2} s^{-1}. The surface concentration of acetylene is taken to be 0.15 mM in water (McAuliffe 1966), in the methane/ethane lakes acetylene concentration is taken to be the same as its mixing ratio in the higher atmosphere (Strobel 2010). Hydrogen, methane, and ethane are assumed to be in equilibrium with the atmosphere. Given these constraints, the biomass calculations for the three conditions mentioned above and the two reactions are given in Table 8.

The values for the biomass predicted for life in liquid methane/ethane are clearly far too high to be in any way acceptable or plausible. We therefore have reason to doubt

[13] See also http://www.ciclops.org/news/making_sense.php?id=6431&js=1.

Table 8
Biomass Surface Density Estimates for Titan in Different Surface Environments

Environment	T (K)	ΔG (kJ mole^{-1})	P_{m_e} (kJ g^{-1} s^{-1})	Biomass (g m^{-2})
$C_2H_2 + 2H_2 \rightarrow C_2H_6$				
Liquid methane/ethane	100	298	1.4×10^{-30}	7.1×10^{22}
Ammonia/water eutectic	176	288	6.3×10^{-15}	1.5×10^{7}
Freezing brine	252	277	1.0×10^{-8}	9.0
$C_2H_2 + 3H_2 \rightarrow 2CH_4$				
Liquid methane/ethane	100	385	1.4×10^{-30}	9.1×10^{22}
Ammonia/water eutectic	176	421	6.3×10^{-15}	2.1×10^{7}
Freezing brine	252	403	1.0×10^{-8}	14

Table 9
References for Field Fluxes Listed in Table 1

Molecule	Ref
CH_3Cl	1–4
COS	5
CS_2	5
DMS	6
H_2S	5
Isoprene	7
N_2O	8
NH_3	...

References. (1) Moore et al. 1996; (2) Dimmer et al. 2001; (3) Cox et al. 2004; (4) Wang et al. 2006; (5) Aneja & Cooper 1989; (6) Morrison & Hines 1990; (7) Fuentes et al. 1996; and (8) Nykanen et al. 1995.

that life that uses chemistry similar to terrestrial life in liquid methane is generating the hydrogen deficit on Titan. An obvious caveat is that Equation (11) based on terrestrial, carbon/water-based life: life operating at 100 K will have radically different, and probably more fragile, chemistry (Bains 2004), and hence different constants in Equation (15).

Life in near-surface water "only" requires a Titan-covering layer between ~1 and 1.5 m thick, equivalent to a modern cabbage farm. A Titan-wide layer of life 1.5 m thick implies a near-surface water layer of at least this thickness across the whole moon, or a thicker layer concentrated in specific regions of the moon, One would have thought that evidence of this would have been detected by IR spectrometry, which it is not (Clark et al. 2010). Again our model suggests that near-surface life is not the sink for atmospheric hydrogen.

Only a modest density of living matter is needed to explain the hydrogen flux if life is present in freezing brine. However, if freezing brine is present, it will be buried under a 100 km thick layer of ice. It is unlikely that gases could exchange with the atmosphere through an ice shell of this sort fast enough to explain the apparent deficit of hydrogen in Titan's atmosphere.

This speculative application of the biomass model illustrates that the model can be used to rule out Earth-like life in some circumstances that are quite unlike Earth. As noted in Section 6.2, there is good reason for our model to apply to other biochemistries based on C, O, N, P, and S. If life on Titan is based on radically different chemistry than Earth's biochemistry, then the constants in Equation (15) will be different, and our model will not accurately predict biomass requirements.

7. SUMMARY

We have created a framework for linking biosignature gas detectability to biomass surface density estimates. This enables us to consider different environments and different biosignature gases than are present on Earth. This liberates predictive atmosphere models from requiring fixed, terracentric biosignature gas source fluxes. We have validated the models on terrestrial production of N_2O/NO, H_2S, CH_4, and CH_3Cl. We have applied the models to the plausibility of NH_3 as a biosignature gas in a reduced atmosphere, to CH_4 on early Earth and present-day Mars, discussed H_2S as an unlikely biosignature gas, and ruled out CH_3Cl as a biosignature gas on Earth or early Earth.

We presented a biosignature gas classification (described in Section 2), needed as a precursor to develop class-specific biomass model estimates. The relevant summary point is that Type I biosignature gases—the by-product gases produced from metabolic reactions that capture energy from environmental redox chemical potential energy gradients—are likely to be abundant but always fraught with false positives. Abundant because they are created from chemicals that are plentiful in the environment. Fraught with false positives because not only does geology have the same molecules to work with as life does, but in one environment where a given redox reaction will be kinetically inhibited and thus proceed only when activated by life's enzymes, in another environment with the right conditions (temperature, pressure, concentration, and acidity) the same reaction might proceed spontaneously. In contrast to Type I biosignature gases, Type III biosignature gases—as chemicals produced by life for reasons other than energy capture or the construction of the basic components of life—are generally expected to be produced in smaller quantities, but will have a wider variety and much lower possibility of false positives as compared to Type I biosignature gases. These qualities are because Type III biosignature gases are produced for organism-specific reasons and are highly specialized chemicals not directly tied to the local chemical environment and thermodynamics.

Model caveats are related to the order of magnitude nature of the biomass estimates, the possible terracentricity of the biomass model estimates, and the lack of ecosystem context.

Exoplanets will have planetary environments and biologies substantially different from Earth's, an argument based on the stochastic nature of planet formation and on the observed variety of planet masses, radii, and orbits. The biomass model estimates are intended to be a step toward a more general framework for biosignature gases, enabling the move beyond the dominant terracentric gases. We hope this new approach will help ensure that out of the handful of anticipated potentially habitable worlds suitable for follow-up spectral observations, we can broaden our chances to identify an inhabited world.

We thank Foundational Questions Institute (FQXI) for providing funding for the seeds of this work many years ago. We thank Matt Schrenk and Bjoern Benneke for useful discussions. W. B. thanks Carl and Barbara Berke for support.

APPENDIX

TERRESTRIAL FLUX REFERENCES

Tables in the Appendix provide the extensive reference list to literature sources of biological field flux and laboratory production rates used in this work.

Table 10
References for Laboratory Fluxes Listed in Table 2

Molecule	Ref
N_2O	1–12
NO	1, 4, 8, 9, 13, 14
H_2S	15–33
CH_4	34–42
CH_3Br	43–51
CH_3Cl	44, 46–53
COS	54–55
CS_2	56
DMS	55, 57–63
Isoprene	64–73

References. (1) Kester et al. 1997; (2) Remde & Conrad 1991; (3) Abouseada & Ottow 1985; (4) Anderson & Levine 1986; (5) Samuelsson et al. 1988; (6) Vorholt et al. 1997; (7) Kaspar 1982; (8) Kesik 2006; (9) Anderson et al. 1993; (10) Wrage et al. 2004; (11) Shaw et al. 2006; (12) Goreau et al. 1980; (13) Lipschultz et al. 1981; (14) Schmidt & Bock 1997; (15) Campbell et al. 2001; (16) Escobar et al. 2007; (17) Stetter & Gunther 1983; (18) Parameswaran et al. 1987; (19) Bottcher et al. 2001; (20) Belkin et al. 1985; (21) Slobodkin et al. 2012; (22) Huber et al. 1987; (23) Brown & Kelly 1989; (24) Belkin et al. 1986; (25) Fardeau et al. 1996; (26) Finster & Thamdrup 1998; (27) Jackson & McInerney 2000; (28) Bak & Pfennig 1987; (29) Bak & Cypionka 1987; (30) Habicht et al. 1998; (31) Widdel et al. 1983; (32) Wallrabenstein et al. 1995; (33) Bolliger et al. 2001; (34) Patel & Roth 1977; (35) Pate et al. 1978; (36) Zeikus et al. 1975; (37) Zinder & Koch 1984; (38) Muller et al. 1986; (39) Pennings et al. 2000; (40) Perski et al. 1981; (41) Schonheit & Beimborn 1985; (42) Takai et al. 2008; (43) Latumus 1995; (44) Dailey 2007; (45) Saemundsdottir & Matrai 1998; (46) Baker et al. 2001; (47) Scarratt & Moore 1998; (48) Laturnus et al. 1998; (49) Manley & Dastoor 1987; (50) Scarratt & Moore 1996; (51) Brownell et al. 2010; (52) Tait & Moore 1995; (53) Harper 1985; (54) Gries et al. 1994; (55) Geng & Mu 2006; (56) Xie et al. 1999; (57) Caron & Kramer 1994; (58) Baumann et al. 1994; (59) Matrai et al. 1995; (60) Ansede et al. 2001; (61) Malin et al. 1998; (62) Stefels & Van Boekel 1993; (63) Gonzalez et al. 2003; (64) Hewitt et al. 1990; (65) Kesselmeier & Staudt 1999; (66) Broadgate et al. 2004; (67) Monson et al. 1994; (68) Wagner et al. 1999; (69) Shaw et al. 2003; (70) Sharkey & Loreto 1993; (71) Logan et al. 2000; (72) Fang et al. 1996; and (73) Harley et al. 1996.

REFERENCES

Abouseada, M. N. I., & Ottow, J. C. G. 1985, Biol. Fertility Soil, 1, 31
Amend, J. P., & Shock, E. L. 2001, FEMS Microbiol. Rev., 25, 175
Anderson, I. C., & Levine, J. S. 1986, ApEnM, 51, 938
Anderson, I. C., Poth, M., Homstead, J., & Burdige, D. 1993, ApEnM, 59, 3525
Anderson, T.-H., & Domsch, K. H. 1989, Soil Biol. Biochem., 21, 471
Aneja, V. P., & Cooper, W. J. 1989, in Biogenic Sulfur in the Environment, ed. E. S. Saltzman & W. J. Cooper (Washington, DC: American Chemical Society), 31
Ansede, J. H., Friedman, R., & Yoch, D. C. 2001, ApEnM, 67, 1210
Arneth, A., Monson, R. K., Schurgers, G., Niinemets, É., & Palmer, P. I. 2008, ACP, 8, 4605
Atreya, S. K., Witasse, O., Chevrier, V. F., et al. 2011, P&SS, 59, 133
Avanier, P., Taoufik, M., Lesage, A., et al. 2007, Sci, 371, 1056
Bahcall, J. N., Pinsonneault, M. H., & Basu, S. 2001, ApJ, 555, 990
Bains, W. 2004, AsBio, 4, 137
Bains, W., & Seager, S. 2012, AsBio, 12, 271
Bak, F., & Cypionka, H. 1987, Natur, 326, 891
Bak, F., & Pfennig, N. 1987, Arch. Microbiol., 147, 184
Baker, J. M., Sturges, W. T., Sunnenberg, J. S., et al. 2001, Chemosphere—Global Change Science, 3, 93
Bakken, L. R., & Olsen, R. A. 1983, ApEnM, 45, 1188
Bar-Nun, A., & Dimitrov, V. 2006, Icar, 181, 320
Baumann, M. E. M., Brandini, F. P., & Staubes, R. 1994, Mar. Chem., 45, 129
Belkin, S., Wirsen, C. O., & Jannasch, H. W. 1985, ApEnM, 49, 1057
Belkin, S., Wirsen, C. O., & Jannasch, H. W. 1986, ApEnM, 51, 1180
Biemann, K., Oro, J., Toulmin, P., III, et al. 1976, Sci, 194, 72
Biemann, K., Oro, J., Toulmin, P., III, et al. 1977, JGR, 82, 4641
Bishop, J. K. B., Davis, R. E., & Sherman, J. T. 2002, Sci, 298, 817
Black, M., Corbineau, F., Gee, H., & Come, D. 1999, Plant Physiol., 120, 463
Bolliger, C., Schroth, M. H., Bernasconi, S. M., Kleikemper, J., & Zeyer, J. 2001, GeCoA, 65, 3289
Borysow, A. 2002, A&A, 390, 779
Bottcher, M. E., Thamdrup, B., & Vennemann, T. W. 2001, GeCoA, 65, 1601
Boyd, P. W., Watson, A. J., Law, C. S., et al. 2000, Natur, 407, 695
Bratbak, G., & Dundas, I. 1984, ApEnM, 48, 755
Brereton, A. J. 1971, Ir. J. Agric. Rese., 10, 185
Broadgate, W. J., Malin, G., Kupper, F. C., Thompson, A., & Liss, P. S. 2004, Mar. Chem., 88, 61
Brown, S. H., & Kelly, R. M. 1989, ApEnM, 55, 2086
Brownell, D. K., Moore, R. M., & Cullen, J. J. 2010, GBioC, 24
Buesseler, K. O., Andrews, J. E., Pike, S. M., & Charette, M. A. 2004, Sci, 304, 414
Campbell, B. J., Jeanthon, C., Kostka, J. E., Luther, G. W., & Cary, S. C. 2001, ApEnM, 67, 4566
Caron, F., & Kramer, J. R. 1994, ScTEn, 45, 11
Cash, W. 2006, Natur, 442, 51
Chandler, S. F., & Thorpe, T. A. 1987, Plant Physiol., 84, 106
Chapman, S. 1930, Mem. Roy. Meteorol. Soc., 3, 103
Clark, R. N., Curchin, J. M., Barnes, J. W., et al. 2010, JGR, 115, E10005
Cox, M. L., Fraser, P. J., Sturrock, G. A., Siems, S. T., & Porter, L. W. 2004, AtmEn, 38, 3839
Dailey, G.-D. 2007, Methyl Halide Production in Fungi (Durham, NH: Univ. New Hampshire)
Dalal, R. C., Allen, D. E., Livesley, S. J., & Richards, G. 2008, Plant Soil, 309, 43
Dartnell, L. R. 2011, AsBio, 11, 551
Davidson, E. A., & Kingerlee, W. 1997, Nutrient Cycling Agroecosystems, 48, 37
Des Marais, D. J., Harwit, M. O., Jucks, K. W., et al. 2002, AsBio, 2, 153
Dimmer, C. H., Simmonds, P. G., Nickless, G., & Bassford, M. R. 2001, Atmos. Chem., 35, 321
Domagal-Goldman, S. D., Meadows, V. S., Claire, M. W., & Kasting, J. F. 2011, AsBio, 11, 419
Escobar, C., Bravo, L., Hernanez, J., & Herrera, L. 2007, Biotechnol. Bioeng., 98, 569
Fang, C., Monson, R. K., & Cowling, E. B. 1996, Tree Physiol., 16, 441
Fardeau, M.-L., Faudon, C., Cayol, J.-L., et al. 1996, Res. Microbiol., 147, 159
Field, C. B., Behrenfeld, M. J., Randerson, J. T., & Falkowski, P. 1998, Sci, 281, 237
Finster, K. 2008, J. Sulfur Chem., 29, 281
Finster, K., Liesack, W., & Thamdrup, B. 1998, ApEnM, 64, 119
Formisano, V., Atreya, S., Encrenaz, T., Ignatiev, N., & Giuranna, M. 2004, Sci, 306, 1758
Fortes, A. D. 2012, P&SS, 60, 10
Friend, A. D., Geider, R. J., Behrenfeld, M. J., & Still, C. J. 2009, in Photosynthesis in silico: Understanding Complexity from Molecules to Ecosystem, ed. A. Laisk, L. Nedbal, & B. V. Govindjee (Dordrecht, The Netherlands: Springer), 465
Fuentes, J. D., Wang, D., Neumann, H. H., et al. 1996, JAtC, 25, 67
Geminale, A., Formisano, V., & Giuranna, M. 2008, P&SS, 56, 1194

Geminale, A., Formisano, V., & Sindoni, G. 2011, P&SS, 59, 137
Geng, C. M., & Mu, Y. J. 2006, AtmEn, 40, 1373
Gerlach, T. 1980, JVGR, 7, 415
Gitelson, A. A., Yacobi, Y. Z., Schalles, J. F., et al. 2000, Arch. Hydrobiol., 55, 121
Gold, T. 1992, PNAS, 89, 6045
Gonzalez, J. M., Covert, J. S., Whitman, W. B., et al. 2003, Int. J. Systematic Evolutionary Microbiol., 53, 1261
Goreau, T. J., Kaplan, W. A., Wofsy, S. C., et al. 1980, ApEnM, 40, 526
Gries, C., NASH, T. H., & Kesselmeier, J. 1994, Biogeochemistry, 26, 25
Guillot, T. 2010, A&A, 520, 27
Haas, J. R. 2010, AsBio, 10, 953
Haber, F. 1913, ZEAPC, 19, 53
Habicht, K. S., Canfield, D. E., & Rethmeier, J. 1998, GeCoA, 62, 2585
Halmer, M. M., Schmincke, M.-U., & Graf, H.-F. 2002, JVGR, 115, 511
Hamilton, H. A., & Bernier, R. 1975, Can. J. Plant Sci., 55, 453
Haqq-Misra, J. D., Domagal-Goldman, S. D., Kasting, P. J., & Kasting, J. F. 2008, AsBio, 8, 1127
Harder, J. 1997, FEMS Microbiol. Ecol., 23, 39
Harley, P., Guenther, A., & Zimmerman, P. 1996, Tree Physiol., 16, 25
Harper, D. B. 1985, Natur, 315, 55
Hewitt, C. N., Monson, R. K., & Fall, R. 1990, Plant Sci., 66, 139
Hitchcock, D. R., & Lovelock, J. E. 1967, Icar, 7, 149
Hoehler, T. A. 2004, Geobiology, 2, 205
Holland, H. D. 1984, The Chemical Evolution of the Atmosphere and Oceans (Princeton, NJ: Princeton Univ. Press)
Hu, R., Seager, S., & Bains, W. 2012, ApJ, 761, 166
Hu, R., Seager, S., & Bains, W. 2013, ApJ, 769, 6
Huber, R., Kristjansson, J. K., & Stetter, K. O. 1987, Arch. Microbiol., 149, 95
Insam, H., & Domsch, K. H. 1988, MicEc, 15, 177
Ishizaka, J., Kiyosawa, H., Ishida, K., Ishikawa, K., & Takahashi, M. 1994, Deep-Sea Res., 41, 1745
Jackson, B. E., & McInerney, M. J. 2000, ApEnM, 66, 3650
Kaltenegger, L., Traub, W. A., & Jucks, K. W. 2007, ApJ, 658, 598
Karl, D. M., Holm-Hansen, O., Taylor, G. T., Tien, G., & Bird, D. F. 1991, Deep-Sea Res., 38, 1029
Kaspar, H. F. 1982, Arch. Microbiol., 133, 126
Kasting, J. F., Eggler, D. H., & Raeburn, S. P. 1993, JG, 101, 245
Kasting, J. F., & Walker, J. C. G. 1981, JGR, 86, 1147
Keppler, F., Harper, D. B., Rockmann, T., Moore, R. M., & Hamilton, J. T. G. 2005, ACP, 5, 2403
Kerr, R. A. 2010, Sci, 330, 26
Kesik, M. 2006, ApMic, 101, 655
Kesselmeier, J., & Staudt, M. 1999, JAtC, 33, 23
Kester, R. A., de Boer, W., & Laanbroek, H. J. 1997, ApEnM, 63, 3872
Kharecha, P., Kasting, J., & Siefert, J. 2005, Geobiology, 3, 53
Kiehl, J. T., & Dickinson, R. E. 1987, JGR, 92, 2991
Kramer, M., & Cypionka, H. 1989, Arch. Microbiol., 151, 232
Krasnopolsky, V. A. 2006, Icar, 185, 153
Krasnopolsky, V. A., & Feldman, P. D. 2001, Sci, 294, 1914
Krasnopolsky, V. A., Maillard, J. P., & Owen, T. C. 2004, Icar, 172, 537
Lang, G. E., Reiners, W. A., & Heier, R. K. 1976, Oecologia, 25, 229
Larson, D. W. 1981, Bryologist, 84, 1
Latumus, F. 1995, Chemosphere, 31, 3387
Laturnus, F., Adams, F. C., & Wiencke, C. 1998, GeoRL, 25, 773
Lawrence, J. R., Korber, D. R., Hoyle, B. D., Costerton, J. W., & Caldwell, D. E. 1991, J. Bacteriol., 173, 6558
Lawson, P. R. 2009, Proc. SPIE, 7440, 744002
Lederberg, J. 1965, Natur, 207, 9
Leger, A., Pirre, M., & Marceau, F. J. 1993, A&A, 277, 309
Le Guern, F., Gerlach, T. M., & Nohl, A. 1982, JVGR, 14, 223
Leliwa-Kopystyński, J., Maruyama, M., & Nakajima, T. 2002, Icar, 159, 518
Lipp, J. S., Morono, Y., Inagaki, F., & Hinrichs, K.-U. 2008, Natur, 454, 991
Lipschultz, F., Zafiriou, O. C., Wofsy, S. C., et al. 1981, Natur, 294, 641
Logan, B. A., Monson, R. K., & Potosnak, M. J. 2000, Trends Plant Sci., 5, 477
Lovelock, J. E. 1965, Natur, 207, 568
MacLulich, J. H. 1987, Mar. Ecol. Prog. Ser., 40, 285
Madhusudhan, N., & Seager, S. 2009, ApJ, 707, 24
Madigan, M. T., Martinko, J. M., & Parker, J. 2003, Brock Biology of Microorganisms (10th ed.; Upper Saddle River, NJ: Prentice-Hall)
Malin, G., Wilson, W. H., Bratbak, G., Liss, P. S., & Mann, N. H. 1998, Limnol. Oceanogr., 43, 1389
Manley, S. L., & Dastoor, M. N. 1987, Limnol. Oceanogr., 32, 709
Matrai, P. A., Vernet, M., Hood, R., et al. 1995, Mar. Biol., 124, 157
McAuliffe, C. 1966, JPhCh, 70, 1267
McKay, C. P., & Smith, H. D. 2005, Icar, 178, 274
Meadows, V., & Seager, S. 2010, in Exoplanets, ed. S. Seager (Tucson, AZ: Univ. Arizona Press:), 441
Miller-Ricci, E., Seager, S., & Sasselov, D. 2009, ApJ, 690, 1056
Mitchell, B. G., Brody, E. A., Holm-Hansen, O., McClain, C., & Bishop, J. 1991, Limnol. Oceanogr., 36, 1662
Monson, R. K., Harley, P. C., Litvak, M. E., et al. 1994, Oecologia, 99, 260
Moore, R. M., Groszko, W., & Niven, S. J. 1996, JGR, 101, 28529
Morrison, M. C., & Hines, M. E. 1990, AtmEn, 24, 1771
Muller, V., Blaut, M., & Gottschalk, G. 1986, ApEnM, 52, 269
Mumma, M. J., Villanueva, G. L., Novak, R. E., et al. 2009, Sci, 323, 1041
Neu, T. R., & Lawrence, J. R. 1997, FEMS Microbiol. Ecol., 24, 11
Nicotri, M. E. 1980, J. Exp. Mar. Biol. Ecol., 42, 13
Nishibayashi, Y., Iwai, S., & Hidai, M. 1998, Sci, 279, 540
Norman, L. H. 2011, A&G, 52, 1.39
Nutzman, P., & Charbonneau, D. 2008, PASP, 120, 317
Nykanen, H., Alm, J., Lano, K., Silvola, J., & Martikainen, P. 1995, J. Biogeography, 22, 351
Ohmoto, H., Watanabe, Y., & Kumazawa, K. 2004, Natur, 429, 395
Olsen, R. A., & Bakken, L. R. 1987, MicEc, 13, 59
Omori, M. 1969, Mar. Biol., 3, 4
Parameswaran, A. K., Provan, C. N., Sturm, F. J., & Kelly, R. M. 1987, ApEnM, 53, 1690
Pate, G. B., Khan, A. W., & Roth, L. A. 1978, J. App. Microbiol., 45, 347
Patel, G. B., & Roth, L. A. 1977, Can. J. Microbiol., 23, 893
Pavlov, A. A., Brown, L. L., & Kasting, J. F. 2001, JGR, 106, 23267
Pavlov, A. A., Kasting, J. F., Brown, L. L., Rages, K. A., & Freedman, R. 2000, JGR, 105, 11981
Pavlov, A. K., Blinov, A. V., & Konstantinov, A. N. 2002, P&SS, 50, 669
Pedersen, K. 1993, ESRv, 34, 243
Pennings, J. L. A., Vermeij, P., de Poorter, L. M. I., Keltjens, J. T., & Vogels, G. D. 2000, Antonie van Leeuwenhoek, 77, 281
Perski, H.-J., Moll, J., & Thauer, R. K. 1981, Arch. Microbiol., 130, 319
Pilcher, C. B. 2003, AsBio, 3, 471
Prieme, A. 1994, Soil Biol. Biochem., 26, 7
Remde, A., & Conrad, R. 1991, FEMS Microbiol. Lett., 80, 329
Ricketts, T. R. 1966, Phytochemistry, 5, 67
Rothman, L. S., Gordon, I. E., Barbe, A., et al. 2009, JQSRT, 110, 533
Saemundsdottir, S., & Matrai, P. A. 1998, Limnol. Oceonogr., 43, 81
Sagan, C., & Mullen, G. 1972, Sci, 177, 52
Samuelsson, M.-O., Cadez, P., & Gustafsson, L. 1988, ApEnM, 54, 2220
Sander, S. P., Friedl, R. R., Abbatt, J. P. D., et al. 2011, Chemical Kinetics and Photochemical Data for Use in Atmospheric Studies (JPL Publication 10-6; Pasadena, CA: JPL)
Scarratt, M. G., & Moore, R. M. 1996, Mar. Chem., 54, 263
Scarratt, M. G., & Moore, R. M. 1998, Mar. Chem., 59, 311
Schmidt, I., & Bock, E. 1997, Arch. Microbiol., 167, 106
Schonheit, P., & Beimborn, D. B. 1985, Eur. J. Biochem., 148, 545
Seager, S. 2010, Exoplanet Atmospheres: Physical Processes (Princeton, NJ: Princeton Univ. Press)
Seager, S., Bains, W., & Hu, R. 2013, ApJ, in press
Seager, S., & Sasselov, D. D. 2000, ApJ, 537, 916
Seager, S., Schrenk, M., & Bains, W. 2012, AsBio, 12, 61
Seager, S., Whitney, B. A., & Sasselov, D. D. 2000, ApJ, 540, 504
Segura, A., Kasting, J. F., Meadows, V., et al. 2005, AsBio, 5, 706
Segura, A., Meadows, V. S., Kasting, J. F., Crisp, D., & Cohen, M. 2007, A&A, 472, 665
Sehmel, G. 1980, AtmEn, 14, 983
Seinfeld, J. H., & Pandis, S. N. 2000, Atmospheric Chemistry and Physics: From Air Pollution to Climate Change (Hoboken, NJ: Wiley)
Selsis, F., Despois, D., & Parisot, J.-P. 2002, A&A, 388, 985
Sharkey, T. D., & Loreto, F. 1993, Oecologia, 95, 328
Shaw, L. J., Nicol, G. W., Smith, Z., et al. 2006, Environ. Microbiol., 8, 214
Shaw, S. L., Chisholm, S. W., & Prinn, R. G. 2003, Mar. Chem., 80, 227
Shen, Q., Dan, H., Chen, Y., & Royse, D. J. 2002, in Mushroom Biology and Mushroom Products, ed. Sánchez et al. (Minneapolis, MN: WSMBMP), 409
Shilov, A. E. 2003, Russian Chem. Bull., 52, 2555
Simon, M., & Azam, F. 1989, Marine Ecol. Prog., 51, 201
Slobodkin, A. I., Reysenbach, A.-L., Slobodkina, G. B., et al. 2012, Int. J. Systematic Evolutionary Microbiol., 62, 2565
Stefels, J., & Van Boekel, W. H. M. 1993, Marine Ecol. Prog., 97, 11
Stetter, K. O., & Gunther, G. 1983, Natur, 305, 309
Strobel, D. F. 2010, Icar, 208, 878
Tait, V. K., & Moore, R. M. 1995, Limnol. Oceanogr., 40, 189
Takai, K., Nakamura, K., Toki, T., et al. 2008, PNAS, 105, 10949
Taran, Y. A., Rozhkov, A. M., Serafimova, E. K., & Esikov, A. D. 1991, JVGR, 46, 255

Tijhuis, L., van Loosdrecht, M. C. M., & Heijnen, J. J. 1993, Biotechnol. Bioeng., 42, 509
Trauger, J. T., & Traub, W. A. 2007, Natur, 446, 771
Vorholt, J. A., Hafenbradl, D., Stetter, K. O., & Thauer, R. K. 1997, Arch. Microbiol., 167, 19
Wagner, W. P., Nemecek-Marshall, M., & Fall, R. 1999, J. Bacteriol., 181, 4700
Wallrabenstein, C., Hauschild, E., & Schink, B. 1995, Arch. Microbiol., 164, 346
Wang, J., Li, R., Guo, Y., Qin, P., & Sun, S. 2006, AtmEn, 40, 6592
Watts, S. F. 2000, AtmEn, 34, 761
Weare, W. W., Dai, X., Byrnes, M. J., et al. 2006, PNAS, 103, 17099
Whitman, W. B., Coleman, D. C., & Wiebe, W. J. 1998, PNAS, 95, 6578
Whittaker, R. H. 1966, Ecology, 47, 103
Widdel, F., Kohring, G.-W., & Mayer, F. 1983, Arch. Microbiol., 134, 286
Williams, E. J., Hutchinson, G. L., & Felsenfeld, F. C. 1992, Glob. Geochem. Cycle, 6, 351
Wong, A. S., Atreya, S. K., Formisano, V., Encrenaz, T., & Ignatiev, N. I. 2004, AdSpR, 33, 2236
Wrage, N., Velthof, G. L., Oenema, O., & Laanbroek, H. J. 2004, FEMS Microbiol. Ecol., 47, 13
Xie, H. X., Scarratt, M. G., & Moore, R. M. 1999, AtmEn, 33, 3445
Yandulov, D. V., & Schrock, R. R. 2003, Sci, 301, 76
Yue, C., Trudeau, M., & Antonelli, D. 2006, Chem. Comms., 18, 1918
Zahnle, K., Haberle, R. M., Catling, D. C., & Kasting, J. F. 2008, JGRE, 113, 11004
Zahnle, K. J. 1986, OrLi, 16, 188
Zeikus, J. G., Weimer, P. J., Nelson, D. R., & Daniels, L. 1975, Arch. Microbiol., 104, 129
Zinder, S. H., & Koch, M. 1984, Arch. Microbiol., 138, 263